INTERNATIONAL TABLES FOR CRYSTALLOGRAPHY

ISSN 1574-8707
it.iucr.org

Volume I, X-ray Absorption Spectroscopy and Related Techniques
ISBN: 978-1-119-43394-1

Chapter 2.1

Keywords: X-ray interactions; X-ray absorption spectroscopy; absorption edges; bound–bound transitions; X-ray scattering; X-ray diffraction.

X-ray interactions with matter

Christopher T. Chantler[a]* and Dudley C. Creagh[b]

[a]School of Physics, University of Melbourne, Melbourne, Australia, and [b]Faculty of Education, Science, Technology and Mathematics, University of Canberra, Canberra, Australia. *Correspondence e-mail: chantler@unimelb.edu.au

This chapter discusses the fundamentals of the interactions of photons and especially X-rays with matter to give an introduction to X-ray absorption spectroscopy (XAS) in its basic form. As such, this chapter uses standard electrodynamics and quantum mechanics, from which the key XAS processes can be defined and presented. Later chapters will develop the theory and applications to old and new experimental fields within the broad umbrella of XAS. Approximations are made in this overview which will be questioned or adapted in later advanced topics. This introduction is predominantly nonrelativistic in development, using only those relativistic terms that are necessary to explain the physical processes.

1. Background

The first indications that spectroscopy could be performed in the X-ray region were seen in the period from 1915 to 1925. From this period until 1975–1985, the best measured X-ray wavelengths and energies had to be expressed in some local unit, most often designated as the xu (× unit) or kxu (kilo × unit). Uncertainty in the conversion factor between the X-ray and optical scales was a dominant contributor to the total uncertainty in the wavelength and energy values of the sharper X-ray emission lines most frequently used in crystallographic experiments. This local unit was generally defined by assigning a specific numerical value to the lattice period of a particular reflection from 'the purest instance' of a particular crystal. Since 1985, the rigorous linking of X-ray wavelengths to visible wavelengths, and hence to SI units and the metre, has been established, allowing greater insight into and understanding of physical processes occurring in the X-ray regime.

The dominant spectra observed from the early years were absorption and absorption edges, characteristic radiation from bound–bound transitions and fluorescence. Characteristic radiation (inner-shell bound–bound transitions) is dominated by the $K\alpha$ spectral doublet across the range of the periodic table. For atomic numbers $Z \geq 10$ these are soft X-ray or X-ray spectra. The two dominant spectral lines, which are usually well resolved, are $K\alpha_1$ for a 1s shell hole being filled with a $2p_{3/2}$ electron and $K\alpha_2$ for a 1s shell hole being filled with a $2p_{1/2}$ electron. Statistical population would naïvely suggest a ratio of integrated area or integrated intensity of 2:1 (Fig. 1). Other strong spectral features are $K\beta$ (Fig. 2), unresolved doublets or multiplets due to a 1s hole being filled by a 3p electron, $L\alpha$ for an $n = 2$ shell hole being filled by an $n = 3$ shell electron *etc.*, and the absorption edges, for example the K edge corresponding to the ionization energy of the 1s electron to the continuum (Fig. 3). Subcomponents of $K\alpha_1$ are labelled $K\alpha_{11}$, $K\alpha_{12}$ *et seq.* and similarly $K\alpha_{21}$, $K\alpha_{22}$ *et seq.* corresponding to fitted spectral energies, amplitudes and widths.

Related chapters

Volume I: 2.4, 2.8, 2.10, 2.12, 2.13, 2.16, 2.19

Usually these components are defined empirically, although the first component is intended to represent the dominant diagram transitions rather than an additional set of satellite transitions with an additional electron hole in upper and lower states from some subshell, for example 3*d*.

This chapter has overlap with several chapters (Chantler *et al.*, 2024; Creagh & Chantler, 2024*a*,*b*; Chantler & Creagh, 2024) of the third edition of *International Tables for Crystallography* Volume C, which supersedes the second edition (Arndt *et al.*, 1999). It leads on to the development of later chapters in this current volume.

2. Types of interaction of X-rays with matter

Across much of the X-ray spectrum, the dominant interaction of a photon with matter is that of *absorption* of the photon via the photoelectric effect, yielding a free photoelectron. Photoelectric absorption (PE) can be represented by a transition amplitude $A^{\rm PE}$ and a cross section in barns per atom $\sigma_{\rm PE} = \tau_{\rm PE}$ (Chantler, 1995, 2000).

Elastic scattering of the photon to yield a second photon wavefunction with the same energy and wavelength in the centre-of-mass frame, scattered through some angle, is the basis of X-ray diffraction (Bragg and Laue) and thermal diffuse scattering (TDS). Elastic scattering becomes more dominant at higher and intermediate X-ray energies. Elastic photon–atom interactions (Crasemann, 1996; Kissell & Pratt, 1985; Kane *et al.*, 1986) include (i) scattering from bound electrons (*Rayleigh scattering*; Lord Rayleigh; Strutt, 1871) with a transition amplitude $A^{\rm R}$ and a cross section in barns per atom $\sigma_{\rm R}$; (ii) scattering from the proton charge in the nucleus (*nuclear Thomson scattering*; Thomson, 1906) with amplitude $A^{\rm NT}$ and cross section $\sigma_{\rm NT}$; (iii) *Delbrück scattering* (Delbrück, 1933; Papatzacos & Mork, 1975; $A^{\rm D}$, $\sigma_{\rm D}$), which is scattering from virtual electron–positron pairs created in the screened nuclear Coulomb potential arising from vacuum polarization and a consequence of quantum electrodynamics; in the photon energy range 100–1000 keV this can be significant at intermediate scattering angles for high-Z targets; and (iv) *nuclear resonance scattering* (Milstein & Schumacher, 1994; $A^{\rm NR}$, $\sigma_{\rm NR}$) from nuclear collective resonances at (much) higher energies. Because these processes yield a photon with indistinguishable properties from the original photon, they are generally coherent and the amplitudes add in phase: $A^{\rm elastic} = A^{\rm R} + A^{\rm NT}$

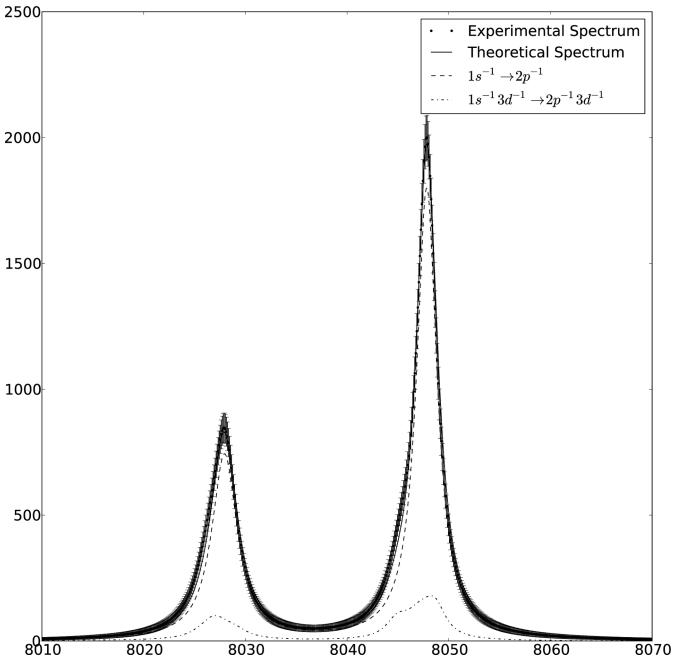

Figure 1
Experimental and theoretical Cu $K\alpha$ X-ray spectra, counts per channel versus energy (keV), with the theoretical contributions to the lines in the diagram ($1s^{-1} - 2p^{-1}$) and those due to the dominant 3*d* satellite from the shake (shake-up) process ($1s^{-1}3d^{-1} - 2p^{-1}3d^{-1}$) predicted separately, showing good agreement at this level. Following Chantler *et al.* (2010).

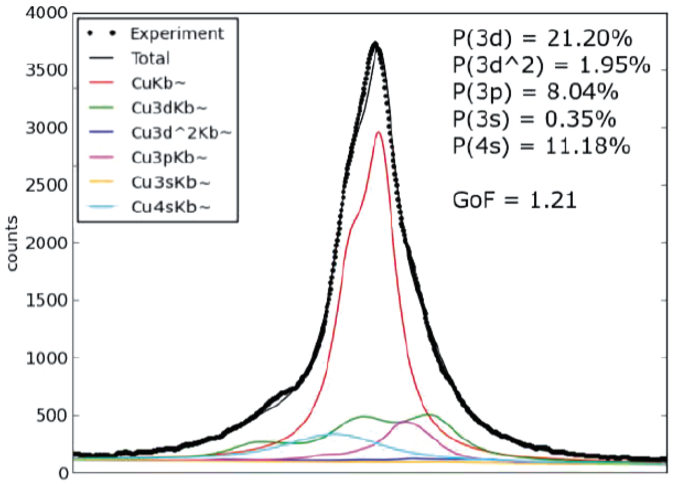

Figure 2
Experimental and theoretical Cu $K\beta$ X-ray spectra, counts per channel versus energy (across the range 8880–8930 eV), with the theoretical contributions to the lines in the diagram ($1s^{-1} - 2p^{-1}$) and those due to the dominant 3*d* satellite from the shake process ($1s^{-1}3d^{-1} - 2p^{-1}3d^{-1}$, 21.20% relative amplitude) and to secondary satellite processes including 4*s* satellites ($1s^{-1}4s^{-1} - 2p^{-1}4s^{-1}$, 11.18% relative amplitude), 3*p* satellites ($1s^{-1}3p^{-1} - 2p^{-1}3p^{-1}$, 1.95% relative amplitude), $3d^2$ satellites ($1s^{-1}3d^{-2} - 2p^{-1}3d^{-2}$, 8.04% relative amplitude) and 3*s* satellites ($1s^{-1}3s^{-1} - 2p^{-1}3s^{-1}$) predicted separately, showing good agreement ($\chi_r^2 = 1.2$) at this level. Following Pham *et al.* (2016).

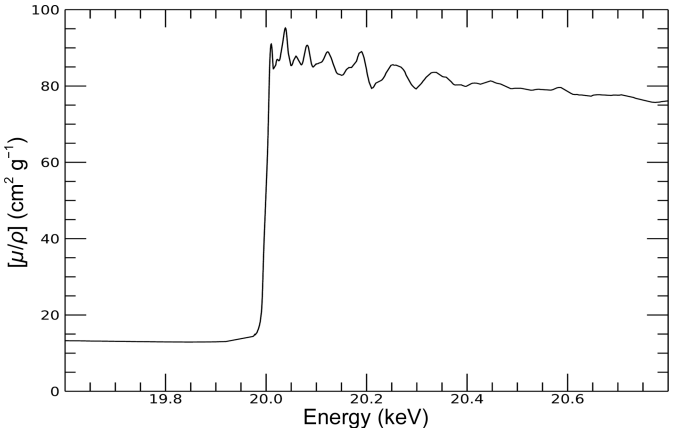

Figure 3
Mo *K* absorption-edge X-ray spectrum showing fine structure. Following de Jonge *et al.* (2005).

$+ A^{D} + A^{NR}$. The total elastic cross section is then proportional to $(A^{elastic})^2$.

Inelastic scattering of the photon leads to an excited state of the atom or molecule with a photon emitted at a lower energy. Inelastic processes become dominant at higher energies. Inelastic photon–atom interactions include (i) *photoexcitation*, including photoabsorption from photoionization, (ii) *Compton scattering* from a free electron and from the electronic wavefunctions of bound electrons (Compton, 1923*a*,*b*; A^{C}, σ_C), (iii) *pair production* of an electron–positron pair from the vacuum field of the nucleus (A^{n}, $\sigma_n = \kappa_n$) with a threshold above $2m_ec^2$ or 1.022 MeV, (iv) pair production in the atomic electron field, *i.e. triplet production* or pair production with electronic excitations (A^{e}, $\sigma_e = \kappa_e$), with a similar threshold, and (v) *photonuclear absorption* (A^{pn}, σ_{pn}) yielding the emission of a neutron $\sigma(\gamma, n)$ or proton $\sigma(\gamma, p)$ or another particle at much higher energies. Assuming that each process is incoherent with every other process yields the common formula $\sigma_{tot} = \sigma_{PE} + \sigma_{elastic} + \sigma_C + \kappa_n + \kappa_e + \sigma_{pn}$.

The separation of elastic and inelastic processes is a little arbitrary since the radiative corrections of quantum electrodynamics, the possibility of emitting very soft photon energies and target recoil effects make 'all' processes inelastic to some extent, while the experimental separation of elastic and inelastic processes are limited by the source bandwidth and the detector resolution.

Photons interact with electric charge. At lower energies, including most X-ray energies, this is dominated by interactions with electrons in matter; at high energies nuclear processes and nuclear resonances become dominant and the photon interacts with the electric charge on the protons in the nucleus. There are also magnetic interactions, but these are normally of secondary importance.

Photon-interaction processes are often defined as *coherent* or *incoherent* in the literature. This is a statement of the coherence of the secondary (photon) wavefunction with that of the primary incident photon. Under normal circumstances the elastic scattering process is coherent, leading to Bragg and Laue X-ray diffraction or thermal diffuse scattering; when each atomic elastic scattering is independent and incoherent with the next this yields the Rayleigh scattering approximation. Similarly, inelastic processes are usually considered to be incoherent; but it is better to ask what degree of coherence they might have either with the incident photon or with other inelastic processes.

The total cross section is dominated by the photoelectric effect (photoabsorption) up to about 6 keV for helium (Fig. 4), 25 keV for carbon (Fig. 5), 80 keV for copper (Fig. 6) and 700 keV for uranium (Fig. 7), increasing with atomic number. This photoelectric absorption (and to a lesser extent Compton scattering) is the precursor and cause of radiation damage to the irradiated medium, which limits the ability of crystallography or X-ray absorption spectroscopy to provide reliable and incisive structural determination. Apart from photoabsorption, elastic processes dominate over inelastic processes up to well above the *K* edge for all atomic numbers (for example ∼10 keV for carbon and perhaps ∼150 keV for

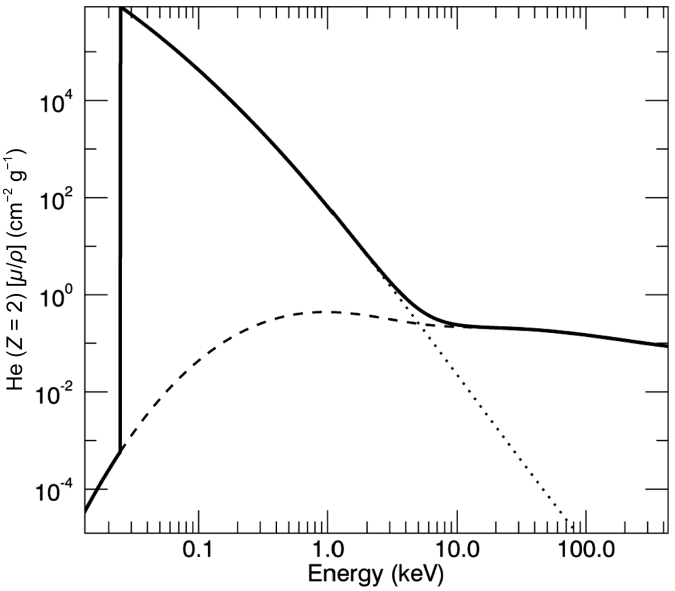

Figure 4
X-ray mass attenuation coefficients $[\mu/\rho]$ in $cm^2\ g^{-1}$ for helium, $Z = 2$. The solid line is the (total) photoelectric mass attenuation coefficient, the dashed line is the dominant photoelectric mass absorption coefficient and the dotted line is the inelastic cross section together with the assumed incoherent atomic elastic cross section. The results are generally in good agreement above 1 keV. Following Chantler (1995, 2000).

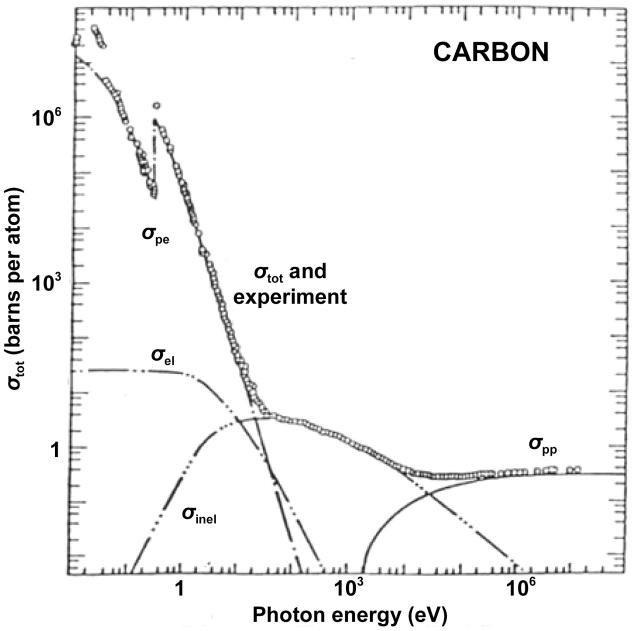

Figure 5
X-ray cross sections for carbon, $Z = 6$, in barns per atom. $[\mu/\rho](Z = 6) = \sigma(Z = 6)/19.9447$. Theoretical cross sections for photon interactions with carbon showing the contributions of photoelectric (dashed/dotted line), elastic (coherent, Rayleigh, dashed/dotted/dotted line), inelastic (incoherent, Compton, dashed/dotted/dotted/dotted line) and pair-production cross sections (solid line) to the total cross sections. Also shown are the experimental data (open circles). Components and totals are generally in good agreement above 1 keV. In comparison with Fig. 4, notice that the level of elastic cross section is nonlinear and is critically dependent on the material, coherence and orientation (Chantler, 1995). From Hubbell *et al.* (1980) and Gerstenberg & Hubbell, 1983).

uranium). Because the elastic processes are usually coherent and may be in phase or out of phase, the material and angular-dependent cross section (for example for Laue–Bragg X-ray diffraction in phase at the Bragg peak region or almost perfectly out of phase for the thermal diffuse scattering magnitude well away from diffraction peaks) can vary by orders of magnitude in different crystalline or noncrystalline materials. Plots from different predictions can differ by factors of two or so, but broad agreement exists above about 1 keV. Computational limitations can be strong at energies below 1 keV and near absorption edges, especially for collective behaviour and nonlinear processes.

All of these cross sections and the functional dependence with energy depend upon the core equations and interactions of electromagnetism and the interaction of electromagnetic fields and photons with matter.

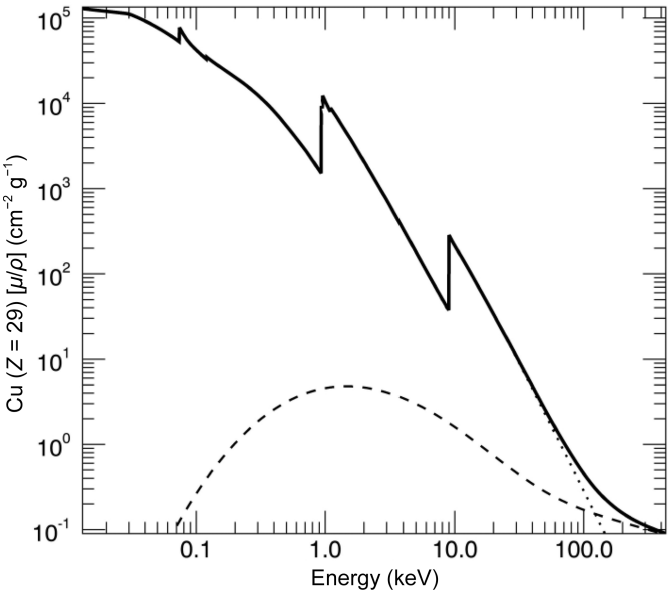

Figure 6
X-ray cross sections for copper, $Z = 29$. Theoretical cross sections for photon interactions with copper metal showing the contributions of photoelectric, elastic (coherent, Rayleigh) and inelastic (incoherent, Compton) processes to 100 keV. The solid line is the (total) photoelectric mass attenuation coefficient, the dashed line is the dominant photoelectric mass absorption coefficient and the dotted line is the inelastic cross section together with the assumed incoherent atomic elastic (Rayleigh) cross section. There is generally good agreement above 1 keV. Following Chantler (1995, 2000).

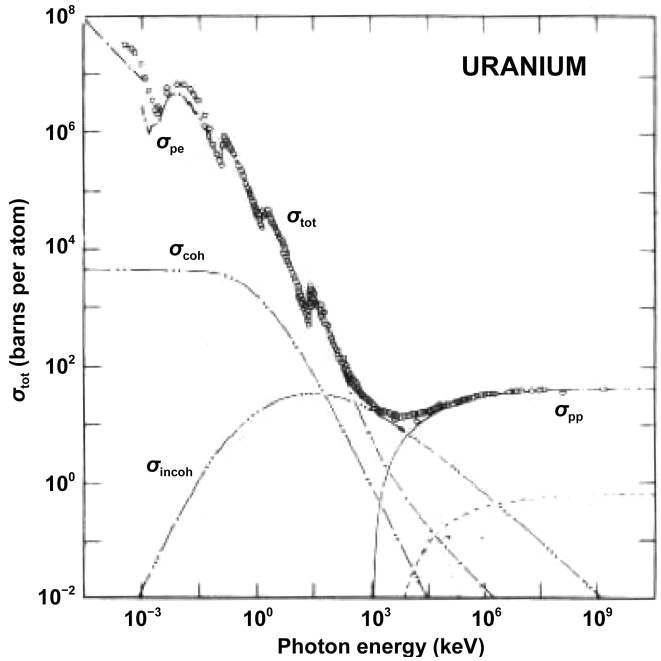

Figure 7
X-ray cross sections for uranium, $Z = 92$. $[\mu/\rho](Z = 92) = \sigma(Z = 92)/395.257$. Labels as per Fig. 5, with an additional triplet cross section (dashed line at high energies). There is generally good agreement above 1 keV. Following Hubbell *et al.* (1980).

3. Electromagnetic interactions

The electromagnetic field is presented in standard undergraduate texts in the D'Alembertian formalism with the electromagnetic tensor, or as the isomorphic representation given here. Both are based on Maxwell's equations in differential form,

$$\begin{aligned}
\nabla \times \mathbf{E} &= -\frac{\partial \mathbf{B}}{\partial t}, \\
\nabla \cdot \mathbf{B} &= 0, \\
\nabla \cdot \mathbf{E} &= \frac{\rho}{\varepsilon_0}, \\
\nabla \times \mathbf{B} &= \mu_0\left(\mathbf{J}_\mathrm{f} + \mathbf{J}_\mathrm{b} + \frac{\partial \mathbf{D}}{\partial t}\right), \\
\rho &= \rho_\mathrm{f} + \rho_\mathrm{b}, \\
\rho_\mathrm{b} &= -\nabla \cdot \mathbf{P}, \\
\mathbf{J}_\mathrm{b} &= \nabla \times \mathbf{M}, \\
\mathbf{D} &= \varepsilon \mathbf{E} = \varepsilon_0 \mathbf{E} + \mathbf{P}, \\
\mathbf{H} &= \mathbf{B}/\mu = \mathbf{B}/\mu_0 - \mathbf{M}. \qquad (1)
\end{aligned}$$

The variables in the equations are the displacement vector $\mathbf{D}$, the free charge density ρ_f, the (total) electric field strength $\mathbf{E}$, the magnetic induction (magnetic flux density) $\mathbf{B}$, the magnetic field strength $\mathbf{H}$ and the free current density $\mathbf{J}_\mathrm{f}$. Constitutive equations are given in terms of the absolute permittivities ε and permeabilities μ (in the medium or in free space ε_0, μ_0) using the total charge density ρ, the bound charge density ρ_b and divergence of polarization $\mathbf{P}$, the total current density $\mathbf{J}$, the bound current density $\mathbf{J}_\mathrm{b}$ and the curl of magnetization $\mathbf{M}$. The wave equation for an electric field in its most general form then follows,

$$\nabla^2 \mathbf{E} = -\nabla\rho/\varepsilon_0 + \mu_0 \frac{\partial \mathbf{J}}{\partial t} + \mu_0 \varepsilon_0 \frac{\partial^2 \mathbf{E}}{\partial t^2} + \mu_0 \frac{\partial^2 \mathbf{P}}{\partial t^2} \qquad (2)$$

and in linear, isotropic and homogeneous media (lih) away from sources we obtain

$$\nabla^2 \mathbf{E} = -\mu\varepsilon \frac{\partial^2 \mathbf{E}}{\partial t^2}. \qquad (3)$$

Similarly, any propagating magnetic field is given by

$$\nabla^2\mathbf{H} = \mu_0\varepsilon_0\frac{\partial^2\mathbf{H}}{\partial t^2} + \mu_0\varepsilon_0\frac{\partial^2\mathbf{M}}{\partial t^2} - \frac{\partial(\nabla\times\mathbf{P})}{\partial t} - \nabla\times\mathbf{J}_\mathrm{f} - \nabla(\nabla\cdot\mathbf{M}),$$
$$\nabla^2\mathbf{B} = -\mu\varepsilon\frac{\partial^2\mathrm{B}}{\partial t^2} \tag{4}$$

in lih media away from sources. Consideration of the vector aspect of an electromagnetic plane-wave solution in free space leads to the transversality of electromagnetic plane waves (**E** is perpendicular to **B** and both are perpendicular to the direction of propagation):

$$\mathbf{E} = -c\hat{\mathbf{n}}\times\mathbf{B}, \quad \mathbf{B} = \frac{1}{c}\hat{\mathbf{n}}\times\mathbf{E}. \tag{5}$$

This is also valid for spherical waves, and shows that both **B** and **E** propagate as transverse waves, in phase, with a speed $c = 1/(\varepsilon\mu)^{1/2}$. In free space this is just the free-space speed of light, while in a dispersive medium this is c/n, where n is the refractive index. The electric and magnetic fields are three-dimensional vectors, so this transversality constrains one of the components but allows the fields to have two orthogonal components of *polarizations* either in a linear basis (linear polarizations) or in a circular basis. The general form of solution to the wave equation is a plane wave or spherical wave or Fourier sum of plane waves of the phasor form

$$\mathbf{E} = \mathbf{E}_0\exp[i(k\cdot r - \omega t)]. \tag{6}$$

Here, k is the wavevector $2\pi/\lambda$ and the phase velocity is $\omega = ck$. The electric and magnetic fields are defined in terms of scalar and vector potentials:

$$\mathbf{E} = -\nabla\varphi - \frac{\partial\mathbf{A}}{\partial t}, \quad \mathbf{B} = \nabla\times\mathbf{A}, \tag{7}$$

There is one degree of freedom in the solution of these equations for the scalar and vector potentials, namely the choice of gauge or the divergence of the vector potential. The two most common gauges used are

$$\text{Coulomb gauge}: \nabla\cdot\mathbf{A} = 0,$$
$$\text{Lorentz gauge}: \nabla\cdot\mathbf{A} = \mu\varepsilon\frac{\partial\varphi}{\partial t}. \tag{8}$$

Substituting the definitions of vector and scalar potentials into the wave equations for electric and magnetic fields gives the self-consistent relations (Bransden & Joachain, 1983; Jackson, 1975; Born & Wolf, 1980)

$$\nabla^2\mathbf{A} - \frac{1}{c^2}\frac{\partial^2\mathbf{A}}{\partial t^2} - \nabla\left(\nabla\cdot\mathbf{A} + \frac{1}{c}\frac{\partial\varphi}{\partial t}\right) = -\frac{4\pi}{c}\mathbf{J}_\mathrm{f},$$
$$\nabla^2\varphi - \frac{1}{c^2}\frac{\partial^2\varphi}{\partial t^2} + \frac{1}{c}\frac{\partial}{\partial t}\left(\nabla\cdot\mathbf{A} + \frac{1}{c}\frac{\partial\varphi}{\partial t}\right) = -4\pi\rho_\mathrm{f}. \tag{9}$$

Within the Lorentz gauge, this reduces to the following inhomogeneous wave equations (in general):

$$\nabla^2\mathbf{A} - \frac{1}{c^2}\frac{\partial^2\mathbf{A}}{\partial t^2} = -\frac{4\pi}{c}\mathbf{J}_\mathrm{f},$$
$$\nabla^2\varphi - \frac{1}{c^2}\frac{\partial^2\varphi}{\partial t^2} = -4\pi\rho_\mathrm{f}. \tag{10}$$

To solve either of these equations we need to find a Green's function as a solution of this second-order inhomogeneous equation, where f is known and given:

$$\nabla^2\Psi - \frac{1}{c^2}\frac{\partial^2\Psi}{\partial t^2} = -4\pi f(\mathbf{r}, t). \tag{11}$$

Decomposing this by a Fourier decomposition into single-frequency components,

$$\Psi(x,y,z,t) = \left(\frac{1}{2\pi}\right)\int_{-\infty}^{\infty}\hat{\Psi}(x,y,z,\omega)\exp(-i\omega t)\,\mathrm{d}\omega,$$
$$f(x,y,z,t) = \left(\frac{1}{2\pi}\right)\int_{-\infty}^{\infty}\hat{f}(x,y,z,\omega)\exp(-i\omega t)\,\mathrm{d}\omega,$$
$$\hat{\Psi}(x,y,z,\omega) = \left(\frac{1}{2\pi}\right)\int_{-\infty}^{\infty}\Psi(x,y,z,t)\exp(i\omega t)\,\mathrm{d}t,$$
$$\hat{f}(x,y,z,\omega) = \left(\frac{1}{2\pi}\right)\int_{-\infty}^{\infty}f(x,y,z,t)\exp(i\omega t)\,\mathrm{d}t, \tag{12}$$

yields the *inhomogeneous Helmholtz wave equation* for each value of ω,

$$(\nabla^2 + k^2)\hat{\Psi}(x,y,z,\omega) = 4\pi\hat{f}(x,y,z,\omega). \tag{13}$$

In order to solve for this, one searches for the corresponding Green's function satisfying

$$(\nabla^2 + k^2)G_k(\mathbf{x},\mathbf{x}') = 4\pi\delta(\mathbf{x}-\mathbf{x}'), \tag{14}$$

If there are no boundary surfaces, this yields a general spherically symmetric solution

$$G_k^{(\pm)}(R) = \frac{\exp(\pm ikR)}{R}, \quad G_k(R) = aG_k^{(+)}(R) + (1-a)G_k^{(-)}(R), \tag{15}$$

where $\mathbf{R} = x - x'$. The first term represents a diverging spherical wave propagating from the origin; the second term is a converging spherical wave. Relative to this, the solution to the inhomogeneous Helmholtz wave equation is

$$\hat{\Psi}(\mathbf{x},\omega) = aG_k^{(+)}(R)\hat{f}(\mathbf{x}',\omega) + (1-a)G_k^{(-)}(R)\hat{f}(\mathbf{x}',\omega). \tag{16}$$

As an illustration, if we construct the corresponding time-dependent Green's functions satisfying

$$\left(\nabla_\mathbf{x}^2 - \frac{1}{c^2}\frac{\partial^2}{\partial t^2}\right)G_k^{(\pm)}(\mathbf{x},t,\mathbf{x}',t') = 4\pi\delta(\mathbf{x}-\mathbf{x}')\delta(t-t'). \tag{17}$$

the solutions are (in k-space) $G_k^{(\pm)}(R) = \exp(i\omega t')$, so by inverse transform the real-space time-dependent Green's function is

$$G^{(\pm)}(R,\tau) = \frac{1}{2\pi}\int_{-\infty}^{\infty}\frac{\exp(\pm ikR)}{R}\exp(-i\omega\tau)\,\mathrm{d}\omega, \quad \tau = t - t'. \tag{18}$$

If k is real, *i.e.* a nondispersive medium, then

$$G^{(\pm)}(R,\tau) = \frac{1}{R}\delta\left(\tau \mp \frac{R}{c}\right)$$

or

$$G^{(\pm)}(\mathbf{x}, t, \mathbf{x}', t') = \frac{\delta\left[t' - \left(t \mp \dfrac{|\mathbf{x} - \mathbf{x}'|}{c}\right)\right]}{|\mathbf{x} - \mathbf{x}'|}.$$

This shows that the Green's function $G^{(+)}$ is the retarded Green's function, exhibiting causality associated with a wave disturbance travelling (outwards) at speed c, while $G^{(-)}$ is the advanced Green's function (possibly from an ingoing, for example, spherical wave). A particular solution, then, to the second-order inhomogeneous [scalar] wave equation is

$$\Psi(\mathbf{x}, t) = \Psi_{\rm in}(\mathbf{x}, t) + \int\int f(\mathbf{x}', t') G^{(\pm)}(\mathbf{x}, t, \mathbf{x}', t')\, \mathrm{d}^3x'\, \mathrm{d}t', \quad (19)$$

where $\Psi_{\rm in}(\mathbf{x}, t)$ is any solution of the homogeneous wave equation for, for example, the incident wave. For $\Psi_{\rm in}(\mathbf{x}, t) = 0$ the solution can be written explicitly as

$$\Psi(\mathbf{x}, t) = \int \frac{f\left[t' - \left(t \mp \dfrac{|\mathbf{x} - \mathbf{x}'|}{c}\right)\right]}{|\mathbf{x} - \mathbf{x}'|}\, \mathrm{d}^3x' = \int \frac{[f(\mathbf{x}', t')]_{\rm ret}}{|\mathbf{x} - \mathbf{x}'|}\, \mathrm{d}^3x', \quad (20)$$

where the square brackets $[f(\mathbf{x}', t')]_{\rm ret}$ refer to the retarded time and retarded potential, yielding integral solutions for the vector and scalar potentials as (Sakurai, 1994)

$$\Phi(\mathbf{x}, t) = \int \frac{\rho\left[t' - \left(t \mp \dfrac{|\mathbf{x} - \mathbf{x}'|}{c}\right)\right]}{|\mathbf{x} - \mathbf{x}'|}\, \mathrm{d}^3x' = \int \frac{[f(\mathbf{x}', t')]_{\rm ret}}{|\mathbf{x} - \mathbf{x}'|}\, \mathrm{d}^3x',$$

$$\mathbf{A}(\mathbf{x}, t) = \int \frac{\mathbf{J}\left[t' - \left(t \mp \dfrac{|\mathbf{x} - \mathbf{x}'|}{c}\right)\right]}{|\mathbf{x} - \mathbf{x}'|}\, \mathrm{d}^3x' = \int \frac{[\mathbf{f}(\mathbf{x}', t')]_{\rm ret}}{|\mathbf{x} - \mathbf{x}'|}\, \mathrm{d}^3x'. \quad (21)$$

That is, the electromagnetic wave will typically be composed of Green's function spherical wavelets arising from a disturbance or source (charge or four-current), causal with respect to the propagation speed of the disturbance (photon wavefield). These derivations are based on the nonrelativistic Green's function with lowest-order relativistic corrections, rather than directly on the Dirac equations with the Dirac (Green's function) propagator, which is however quite similar (Sakurai, 1967). Green's function approaches are basic for the understanding of X-ray absorption fine structure (XAFS) and will be developed in numerous cases in later chapters.

The idea of a Green's function as a source of an outgoing wave in an interaction leads naturally to the idea of an oscillator of charge, yielding a Green's function source term in a response function such as an outgoing photon wave, as discussed in the next section.

4. Oscillators, absorption and absorption edges

The Lorentz force law indicates that charge will respond to electromagnetic fields, and that charge will *oscillate* in response to periodic electromagnetic fields. In many stable potentials a system (atom, molecule, solid) is locally neutral, and so an excursion of electric charge leads to a restoring force following Hooke's law and simple harmonic motion. Consider initially an electron experiencing a Lorentz force from the (effective) fields $\mathbf{E}'$ and $\mathbf{B}'$, to first order neglecting the magnetic field compared with the electric field. The nuclear potential may naïvely be assumed to give a linear, elastic restoring force for small field oscillations. The equation of motion is then

$$\mathbf{F} = e\mathbf{E}' + e\mathbf{v} \times \mathbf{B}' - q\mathbf{r} = m\ddot{\mathbf{r}}, \quad \mathbf{E}' = \mathbf{E}'_0 \exp(-i\omega t). \quad (22)$$

Neglecting $\mathbf{B}'$ and assuming a phasor solution for the charge oscillator position $\mathbf{r}$ gives

$$\mathbf{r} = \mathbf{r}_0 \exp(-i\omega t) = \frac{e\mathbf{E}'}{m(\omega_0^2 - \omega^2)}, \quad \omega_0 = \left(\frac{q}{m}\right)^{1/2}, \quad (23)$$

where ω_0 is the resonance or absorption frequency. Each electron contributes to the total electric dipole moment per unit volume and hence polarization

$$\mathbf{P} = N\mathbf{p} = Ne\mathbf{r} = N\frac{e^2}{m}\frac{\mathbf{E}'}{(\omega_0^2 - \omega^2)} = N\alpha\mathbf{E}', \quad (24)$$

where α is the *polarizability* and is a second-rank tensor, but it may be taken here to be the mean polarizability or the polarization per electron (or oscillator), assuming that the system is isotropic and that there are no permanent dipole moments in the absence of a field. N is the number of electrons per unit volume. From the definition of the refractive index as the ratio of the velocity in the vacuum, c, to that in the medium,

$$n = \frac{c}{v} = \left(\frac{\varepsilon\mu}{\varepsilon_0\mu_0}\right)^{1/2} = c(\varepsilon\mu)^{1/2} = (\varepsilon_r\mu_r)^{1/2}. \quad (25)$$

Following equation (24), we need to determine the 'effective field' $\mathbf{E}'$ on the oscillating electron relative to the actual (mean) electric field $\mathbf{E}$. The problem is that the local electron oscillators which give the polarization do not see the mean electric field. For example, the local oscillator will be affected by some of the surrounding dipoles, but (or and) one should not count the dipole of the local oscillator itself. If we define a sphere outside the electron (where the electronic wavefunction is negligible), outside of which there is the uniform mean field and polarization of the medium (and where the local structure is irrelevant), and inside of which is a vacuum, then we can consider the field modified by the medium but isolated from the effect of the local electron (dipole). The effect on the (scalar) potential of the near region is zero for a physically random distribution of, for example, molecules or dipoles. Hence, the (scalar) potential at the centre (*i.e.* at the dipole in question) can be modelled by considering the potential of the complementary configuration, *i.e.* a spherical dielectric region surrounded by free space. This complementary potential at the origin is exactly opposite to the original potential: the sum of the two potentials is that due to a uniform homogeneously polarized material with no boundary, so that the impact of the surrounding charge densities for the retarded potentials may be used. This is the same as saying that the effect of the surrounding dielectric is the opposite of that for a uniformly polarized sphere, which is a standard undergraduate problem.

With minor effort (Born & Wolf, 1980; Hecht & Zajac, 1979) we can use the standard electromagnetism solution for the polarization, defining the dielectric susceptibility η,

$$\mathbf{E}' = E + \frac{P}{3\varepsilon_0}, \quad P = \eta\varepsilon_0 E, \tag{26}$$

leading to the Lorenz–Lorentz (n^2) or Clausius–Mosotti (ε_r) equation for the relation between an external, incident wavefield and its action upon a local oscillator embedded within a dielectric medium,

$$n^2 \simeq \frac{\varepsilon}{\varepsilon_0} = \varepsilon_r = 1 + \eta = \frac{1 + \dfrac{2N\alpha}{3}}{1 - \dfrac{N\alpha}{3}},$$
$$\alpha = \frac{3\varepsilon_0}{N}\frac{\varepsilon_r - 1}{\varepsilon_r + 2} = \frac{3\varepsilon_0}{N}\frac{n^2 - 1}{n^2 + 2}. \tag{27}$$

In the visible regime this local environment effect can be very significant, as $n^2 \simeq 1.4$ is common; in the X-ray regime $n^2 \simeq 1 - 0.0000002$, so $n^2 + 2 \simeq 3$ to a very good approximation and one recovers the simpler and standard equations. However, thinking more broadly about the problem: in the infrared regime (say 400–1200 cm^{-1}), with infrared and vibrational spectroscopy for molecules, solids, biological systems *etc.*, the refractive index can easily correspond to an enormous relative permittivity of 2.21 (dioxan), 7.43 (tetrahydrofuran), 8.93 (dichloromethane) or 35.69 (acetonitrile, corresponding to $n^2 \simeq 36$). These are not constant as functions of energy. This explains why and how some materials make good lenses, some make high-index lenses and what their range of applicability is. The answer lies directly and explicitly in the resonances of the oscillator strength, or equivalently in the (atomic, plasmonic or effective) form factors and combined structure factors of materials.

Very often, only a relativistic equation can explain the behaviour, the origin and the location of the resonances. This expands the derivation and definition of refractive index, permittivity and (X-ray) (atomic) form factor from high energies down to the visible region and below. It also shows explicitly the limits of the notions used in both crystallography and X-ray absorption spectroscopy.

If a magnetic system were involved, then we would in an identical manner obtain

$$\mathbf{B}' = \mathbf{B} - \frac{\mu_0 \mathbf{M}}{3}, \quad \mathbf{M} = \chi_\mathrm{m}\mathbf{H} = \frac{\chi_\mathrm{m}}{\mu}\mathbf{B}. \tag{28}$$

Even in the X-ray regime it is not normally possible to identify μ_r or χ_m at an electronic, oscillator or atomic level because the collective motions in magnetic systems dominate. For example, diamagnetic materials have $\mu_r \simeq 1 - 10^{-5}$ and paramagnetic materials have $\mu_r \simeq 1 + 10^{-5}$, but conventionally magnetic systems (ferromagnetism, ferrimagnetism *etc.*) have a tensorial $(\mu_r)_{ij}(T,$ history$) \simeq 10^2 \rightarrow 10^6$ from macroscopic or microscopic aligned domains, which is a function of the temperature and history of the sample. In general, therefore,

$$n \simeq \left(\frac{\varepsilon\mu}{\varepsilon_0\mu_0}\right)^{1/2} = (\varepsilon_r\mu_r)^{1/2} = \left[\mu_r\left(\frac{1 + \dfrac{2N\alpha}{3\varepsilon_0}}{1 - \dfrac{N\alpha}{3\varepsilon_0}}\right)\right]^{1/2}$$
$$= \left[\mu_r\left(\frac{1 + \dfrac{e^2}{m\varepsilon_0}\dfrac{2N}{3(\omega_0^2 - \omega^2)}}{1 - \dfrac{e^2}{m\varepsilon_0}\dfrac{N}{3(\omega_0^2 - \omega^2)}}\right)\right]^{1/2}. \tag{29}$$

If we assume that $\mathbf{E}' = \mathbf{E}$ [where $\mathbf{E}$ is the (total) electric field at point $\mathbf{x}$], then we can relate the displacement vector $\mathbf{D}$ to that of $\mathbf{E}$ following

$$\mathbf{D} = \varepsilon\mathbf{E} = \varepsilon_0\mathbf{E} + \mathbf{P} = \varepsilon_0 E\left(1 + \frac{N\alpha}{\varepsilon_0}\right), \tag{30}$$

and, neglecting the permeability,

$$n \simeq \left(\frac{\varepsilon}{\varepsilon_0}\right)^{1/2} = \left(1 + \frac{N\alpha}{\varepsilon_0}\right)^{1/2} = \left(1 + \frac{e^2}{m\varepsilon_0}\frac{N}{(\omega_0^2 - \omega^2)}\right)^{1/2}. \tag{31}$$

If we include the necessary damping (excited-state lifetime) term in the bound field of the nucleus (or the molecule or the solid ...), then we generalize the force to

$$\mathbf{F} = e\mathbf{E}' - q\mathbf{r} - \gamma\dot{\mathbf{r}} = m\ddot{\mathbf{r}}, \quad \mathbf{E}' = \mathbf{E}'_0\exp(-i\omega t), \tag{32}$$

$$\mathbf{r} = \mathbf{r}_0\exp(-i\omega t) = \frac{e\mathbf{E}'}{m(\omega_0^2 - \omega^2) - i\omega\gamma}, \quad \omega_0 = \left(\frac{q}{m}\right)^{1/2}, \tag{33}$$

$$n \simeq \left(1 + \frac{e^2}{m\varepsilon_0}\frac{N}{(\omega_0^2 - \omega^2) - i\omega\gamma/m}\right)^{1/2}. \tag{34}$$

For the general case there are many such resonant frequencies with different amplitudes or oscillator strengths, yielding

$$n \simeq \left(1 + \frac{e^2}{m\varepsilon_0}\sum_k \frac{N_k}{(\omega_k^2 - \omega^2) - i\omega\kappa_k}\right)^{1/2}, \quad \kappa_k = \gamma_k/m. \tag{35}$$

In the X-ray regime, or where the refractive index is $1 - 10^{-7}$, this may be given to a very good approximation by the first-order Taylor series expansion

$$n \simeq 1 - \frac{e^2}{2m\varepsilon_0}\sum_k \frac{N_k}{(\omega_k^2 - \omega^2) - i\omega\kappa_k}. \tag{36}$$

This corresponds to a sum, with a scale, of the effective number of charge (electron) oscillators in the matter. The form factor in physics is defined as the scattering power relative to a free particle; for an electron this is the scattering power (the oscillator amplitudes) as a function of momentum transfer and frequency, relative to the Thomson scattering power for a free electron. For an atom dominated by electron scattering, this approaches Z in the limit of high frequency where the electrons are nearly free, corresponding to the number of electrons in the atom.

This can be seen as a sum over electrons each with unit oscillator strength, yet the same equation can describe effective plasmon oscillators in a condensed matter or band-structure computation down to visible energies. An effective

plasmon oscillator is just like an electron but may have fractional or effective charge. The sum of all plasmon strengths should still give the total number of electrons by conservation of charge. Hence, in the X-ray regime this expression may be re-expressed as a simple sum of real and complex components, defining the (X-ray) (atomic) form factor,

$$n \simeq 1 - \delta - i\beta = 1 - \frac{r_0}{2\pi}\lambda^2 \sum_k N_k f_k. \tag{37}$$

The (X-ray) (atomic) form factor represents the photon scattering factor (of an atom) relative to that of a (Thomson) free electron,

$$\begin{aligned} f\left(\mathbf{q} = \mathbf{k}_\mathrm{f} - \mathbf{k}_\mathrm{i} = \frac{2\omega \sin(\theta/2)}{c}\hat{\mathbf{q}}, \omega\right) \\ = \int \rho(r) \exp[i(\mathbf{k}_\mathrm{f} - \mathbf{k}_\mathrm{i}) \cdot \mathbf{r}]\, \mathrm{d}V \simeq \sum_k \frac{N_k \omega^2}{(\omega^2 - \omega_k^2) - i\omega\kappa_k}, \\ f(\mathbf{q} = \mathbf{k}_\mathrm{f} - \mathbf{k}_\mathrm{i}, \omega) = \mathrm{Re}(f) + i\mathrm{Im}(f) = f_0 + f' + if'', \\ \sum_k N_k = Z. \end{aligned} \tag{38}$$

The form factor has absorptive (imaginary) components and scattering (real) components. The scattering component depends upon the angle of incidence $\theta/2$ and the scattering angle θ, so that $\mathbf{q}$ (or $\mathbf{K}$) is the change of wavevector (momentum/$\hbar$) of the photon upon scattering and $\mathbf{q} = 0$ implies scattering in the forward direction. Each atomic subshell will represent a separate type of oscillator with a separate resonant energy, which is therefore the absorption edge for the photoelectron from that subshell. In the X-ray regime, the *mass absorption coefficient* $[\mu/\rho]$ is then given by

$$\begin{aligned} I = I_0 \exp\left(-\left[\frac{\mu}{\rho}\right](\rho t)\right), \quad \left[\frac{\mu}{\rho}\right] = \frac{4\pi\beta}{\rho\lambda}, \\ \beta = \frac{r_0}{2\pi}\lambda^2 \mathrm{Im}[f(\omega, 0)] \simeq \frac{e^2}{2m\varepsilon_0} \sum_k \frac{N_k \kappa_k \omega}{(\omega^2 - \omega_k^2)^2 + \omega^2 \kappa_k^2}. \end{aligned} \tag{39}$$

One of the most important consequences of this for the computation and self-consistency of form factors is the causal link between the real and imaginary components of this complex function by the Kramers–Kronig transforms, where **P** represents the Cauchy principal value:

$$\begin{aligned} f'(\omega, \mathbf{q} = \mathbf{k}_\mathrm{f} - \mathbf{k}_\mathrm{i} = 0) = \frac{2}{\pi}\mathbf{P}\int_{\omega_k}^{\infty} \frac{\omega' f''(\omega', 0)}{\omega^2 - \omega'^2}\, \mathrm{d}\omega', \\ f''(\omega, \mathbf{q} = \mathbf{k}_\mathrm{f} - \mathbf{k}_\mathrm{i} = 0) = -\frac{2}{\pi}\mathbf{P}\int_{0}^{\infty} \frac{f'(\omega', 0)}{\omega^2 - \omega'^2}\, \mathrm{d}\omega', \\ \mathrm{Im}[f(\omega, 0)] = f''(\omega, 0) = \frac{\omega \sigma_\mathrm{PE}(\omega)}{4\pi r_\mathrm{e} c}. \end{aligned} \tag{40}$$

These are linked to related Kramers–Kronig transforms and to sum rules for oscillators, usually requiring a detailed quantum-mechanical basis.

5. Quantum-mechanical basis of photon interaction: time-dependent perturbation theory

In the preceding section, we addressed the question of the nature of the interaction of photons with electrons within the framework of classical electromagnetism. The electrons were assumed to be bound by potentials and to react with the incoming wavefield as an oscillator with a natural frequency ω_k driven by the electromagnetic fields associated with a photon with a frequency ω. This led to equations (38), (39) and (40), which are very important equations in crystallography, giving expressions for the *atomic form factor f*, the *dispersion corrections* f' and f'', the relation between f' and f'' (the Kramers–Kronig relation) and the relation between f'' and the photoelectric component of the atomic scattering cross section μ_PE. Not so apparent from equations (39) and (40) is a term representing the damping constant for the classical driven oscillator [$\exp(i\omega_k)$], which is explicit in equation (38). In a real system this term represents the radiative line width (Chantler *et al.*, 2024) and is insignificant unless the incoming photon has an angular frequency close to the resonant frequency.

From the understanding of the photoelectric effect, the photon is a quantum of the electromagnetic field, a particle with an oscillating electric and magnetic field propagating from the source through an experimental or optical path to absorption, scattering or detection. Following the minimal substitution prescription for the Schrödinger equation $\mathbf{p} \rightarrow \mathbf{p} - q\mathbf{A}$, $V \rightarrow V + q\varphi$ with the electron charge $q = -e$, including spin from the relativistic corrections of the first-order Pauli reduction of the Dirac equation (Sakurai, 1967), and a term beyond the Pauli reduction (Blume, 1994; Vettier, 1994; Blume, 1985), we have

$$\begin{aligned} \mathbf{H} &= \frac{(\mathbf{p} + e\mathbf{A})^2}{2m} + \frac{e\mathbf{S} \cdot \mathbf{B}}{m} - \frac{e^2}{2m(mc^2)}\mathbf{S} \cdot [\dot{\mathbf{A}}(\mathbf{r}) \times \mathbf{A}(\mathbf{r})] + V - e\varphi \\ &= \frac{\mathbf{p}^2}{2m} + V + \frac{e}{2m}(\mathbf{p} \cdot \mathbf{A} + \mathbf{A} \cdot \mathbf{p}) + \frac{e^2 \mathbf{A} \cdot \mathbf{A}}{2m} + \frac{e\mathbf{S} \cdot \mathbf{B}}{m} \\ &\quad + \frac{e^2}{2m(mc^2)}\mathbf{S} \cdot [\dot{\mathbf{A}}(\mathbf{r}) \times \mathbf{A}(\mathbf{r})] \\ &= \mathbf{H}_0 + \mathbf{H}', \end{aligned} \tag{41}$$

where **p** is the charge (electron) momentum, **S** is the particle (electron) spin and V is the potential energy. Note that the last two terms are higher-order relativistic reductions from the Dirac equation. We would need additional corrections for the relativistic and quantum electrodynamical corrections for the energy eigenvalues and eigenfunctions to achieve higher accuracy, so that for example

$$\frac{e\mathbf{S} \cdot \mathbf{B}}{m} \rightarrow \frac{g_s e\mathbf{S} \cdot \mathbf{B}}{2m} \ldots,$$

but the present prescription suffices for most current work relating to XAFS. The unperturbed, time-independent (non-relativistic) Hamiltonian and stationary-state eigenfunctions and eigenvalues are defined by

$$\mathbf{H}_0 = \frac{\mathbf{p}^2}{2m} + V, \quad i\hbar\frac{\partial}{\partial t}\psi_k = \mathbf{H}_0\psi_k = E_k\psi_k. \tag{42}$$

The time-independent Hamiltonian yields an (infinite) series of nondegenerate and degenerate levels which will exist forever (*i.e.* they are stable eigenfunctions) in an isolated system. In such a system, it is generally impossible to (i) have an observer, (ii) have a human/biological enquirer, (iii) have any detector and ergo (iv) investigate any property of this system. This is not exactly to say that any measurement of a system collapses its wavefunction: in principle the system may have already been in a pure eigenstate and therefore will not change its state. Nor is the issue that the system should include the more complex and complete detector/enquirer/observer: in most cases this would seem ridiculous to model. Principally, any (detection) event is necessarily that: localized in space and time and therefore time-dependent. Time-dependent Hamiltonians allow time-dependent solutions, and hence the ability of the detailed state of the system to change. Any (particle physics or condensed-matter physics) scattering event is a key example of a process that therefore requires time-dependence of the Hamiltonian to explain any results. Most of the time, we use assumptions based on perturbation theory in order to discuss these principles, and it is very convenient to do so here.

In the general time-dependent Hamiltonian we invoke perturbation theory to yield general solutions for the final-state wavefunctions as an ordered iteration from initial-state wavefunctions and coefficients in the Fermi *interaction picture*. Formally, we invoke perturbation theory wherever $\mathbf{H}' \ll \mathbf{H}_0$. Following, for example, Sakurai (1967) or many others, with $\Psi_0 = \sum_k c_k^{(0)}|\psi_k\rangle \exp(iE_kt/\hbar)$ and $\Psi(t) = \sum_k c_k(t)|\psi_k\rangle \exp(iE_kt/\hbar)$, leads to the *variation of constants method* $c_k(t) = c_k^{(0)} + \sum_s \lambda^i c_k^{(s)}(t)\ldots$ with the iterative solution to convergence of $\dot{c}_j^{(s+1)}(t) = (1/i\hbar)\sum_k c_k^{(s)}(t)\langle\psi_j|\mathbf{H}'(t)|\psi_k\rangle \exp(i\omega_{jk}t)$. This is equivalent to the *evolution operator (matrix)* $\mathbf{U}(t, t') = [u_{ij}(t, t')]$ for the array of coefficients $\mathbf{C}(t) = [c_j(t)]$ with $\Psi(t') = \mathbf{U}(t, t')\Psi(t)$, $\mathbf{C}(t') = \mathbf{U}(t, t')\mathbf{C}(t)$ with initial (infinitesimal) conditions

$$\mathbf{U}(t, t') = \begin{cases} \mathbf{1}, & t = t' \\ \dot{\mathbf{C}}(t) & t' - t = \delta t \end{cases}.$$

Hence, in a time-dependent system $\dot{\mathbf{C}}(t') = (1/i\hbar)\mathbf{H}'(t)\mathbf{C}(t)$ and $\dot{\mathbf{U}}(t', t) = (1/i\hbar)\mathbf{H}'(t)\mathbf{U}(t, t')$, yielding the recursive $\dot{\mathbf{U}}(t', t) = (1/i\hbar)\int_t^{t'} \mathbf{H}'(\tau)\mathbf{U}(t, \tau)\,\mathrm{d}\tau$ with the *Fredholm/Dyson iterative series* solution

$$\dot{\mathbf{U}}(t', t) = \frac{1}{i\hbar}\int_t^{t'}\mathbf{H}'(\tau)\,\mathrm{d}\tau + \left(\frac{1}{i\hbar}\right)^2\int_t^{t'}\mathbf{H}'(t_1)\,\mathrm{d}t_1\int_t^{t_1}\mathbf{H}'(t_2)\,\mathrm{d}t_2 + \ldots \tag{43}$$

From the earlier section, we can invoke a second illustration of Green's function as the kernel of an integral operator, the propagator of a time-dependent wavefunction, involving the Green's function for a Hamiltonian function of energy, linking directly to *Fermi's golden rule*, for example

$$\left(\frac{\hbar^2}{2m}\nabla_{\mathbf{r}'}^2 + V(\mathbf{r}') - i\hbar\frac{\partial}{\partial t}\right)G_k^{(\pm)}(\mathbf{r}, t, \mathbf{r}', t') = 4\pi\delta(\mathbf{r} - \mathbf{r}')\delta(t - t'). \tag{44}$$

Then, for causal propagation one again chooses the time-retarded Green's function or propagator

$$\begin{aligned} G^{(+)}(\mathbf{r}, t, \mathbf{r}', t') &= \left\langle \mathbf{r}' \middle| \exp\left(\frac{-i\hat{H}(t' - t)}{\hbar}\right)\middle| \mathbf{r}\right\rangle \\ &= \left\langle \mathbf{r}' \middle| \left\{\sum_k |k\rangle \exp\left(\frac{-iE_k(t' - t)}{\hbar}\right)\langle k|\right\}\middle| \mathbf{r}\right\rangle, \end{aligned} \tag{45}$$

from which a formal solution is the *Lippmann–Schwinger equation*,

$$\mathbf{\Psi}(k, \mathbf{r}) = \mathbf{\Phi}(k, \mathbf{r}) + \int G_0(k, \mathbf{r}, \mathbf{r}')V(\mathbf{r}')\mathbf{\Psi}(k, \mathbf{r}')\,\mathrm{d}r' \tag{46}$$

or

$$\mathbf{\Psi}(\mathbf{r}, t) = \mathbf{\Phi}(\mathbf{r}, t) + \int G_0(\mathbf{r}, \mathbf{r}')\mathbf{H}'(\mathbf{r}', t')\mathbf{\Psi}(\mathbf{r}', t')\,\mathrm{d}\mathbf{r}'\,\mathrm{d}t', \tag{47}$$

where $\mathbf{\Phi}$ is the incident wave and $G_0(k, \mathbf{r}, \mathbf{r}') = G^{(+)}(|\mathbf{r} - \mathbf{r}'|) = -[\exp(ik|\mathbf{r} - \mathbf{r}'|)]/(4\pi|\mathbf{r} - \mathbf{r}'|)$, which can be transformed into an integral equation for the Green's function

$$G^{(+)}(\mathbf{r}, \mathbf{r}') = G_0^{(+)}(\mathbf{r}, \mathbf{r}') + \int G_0^{(+)}(\mathbf{r}, \mathbf{r}'')V(\mathbf{r}'')G^{(+)}(\mathbf{r}'', \mathbf{r}')\,\mathrm{d}\mathbf{r}'' \tag{48}$$

as a special case of the *Dyson equation*. In turn, this can be expanded into a *Born sequence*,

$$\begin{aligned} &\Psi(\mathbf{r}, t) = \psi_n(\mathbf{r}, t), \quad \psi_0(\mathbf{r}, t) = \Phi(\mathbf{r}, t), \\ &\psi_1(\mathbf{r}, t) = \Phi(\mathbf{r}, t) + \int G_0^{(+)}(\mathbf{r}, t, \mathbf{r}', t')H'(\mathbf{r}', t')\Phi(\mathbf{r}', t')\,\mathrm{d}\mathbf{r}'\,\mathrm{d}t', \\ &\psi_n(\mathbf{r}, t) = \Phi(\mathbf{r}, t) + \int G_0^{(+)}(\mathbf{r}, t, \mathbf{r}', t')H'(\mathbf{r}', t')\psi_{n-1}(\mathbf{r}', t')\,\mathrm{d}\mathbf{r}'\,\mathrm{d}t'. \end{aligned} \tag{49}$$

We can define the time integral $G(t)$ by setting $t' = 0$ and $\mathbf{r}' = \mathbf{r}$ in equation (45):

$$\begin{aligned} G(t) &= \int \mathrm{d}\mathbf{r}' G^{(+)}(\mathbf{r}', t; \mathbf{r}', 0) \\ &= \int \mathrm{d}\mathbf{r}' \sum_{a'} |\langle \mathbf{r}'|a'\rangle|^2 \exp\left(\frac{-iE_{a'}t}{\hbar}\right) = \sum_{a'} \exp\left(\frac{-iE_{a'}t}{\hbar}\right) \end{aligned}$$

for the basis set $|a'\rangle$ or k. The Fourier transform of $G(t)$ is

$$\begin{aligned} G^{(+)}(E) &= -\frac{i}{\hbar}\int_o^\infty G(t)\exp\left(\frac{iEt}{\hbar}\right)\mathrm{d}t \\ &= -\frac{i}{\hbar}\int_o^\infty \sum_k \exp\left(\frac{-iE_kt}{\hbar}\right)\exp\left(\frac{iEt}{\hbar}\right)\mathrm{d}t \\ &= \sum_k \frac{1}{E - E_k + i\varepsilon}, \end{aligned} \tag{50}$$

where the oscillating integral is made meaningful by the off-axis contour (or damping coefficient) with $E \rightarrow E + i\varepsilon$. In the limit $\varepsilon \rightarrow 0$, this is a sum of the resonant eigenvalue poles. This is equivalent to the Lippmann–Schwinger equation for the transition amplitude $\mathbf{T}$ in terms of the potential $\mathbf{V}$:

$$\begin{aligned}\mathbf{T} &= \mathbf{V} + \mathbf{V}\frac{1}{E - H_0 + i\varepsilon}\mathbf{T} \\ &= \mathbf{V} + \mathbf{V}\frac{1}{E - H_0 + i\varepsilon}\mathbf{V} \\ &\quad + \mathbf{V}\frac{1}{E - H_0 + \varepsilon}\mathbf{V}\frac{1}{E - H_0 + i\varepsilon}\mathbf{V} + \ldots \end{aligned} \tag{51}$$

Phenomenologically, this is equivalent to a wave (i) created by the potential $V(\mathbf{r})$ at $\mathbf{r}$, (ii) propagated to $\mathbf{r}'$ by the propagator, (iii) scattered by the potential $V(\mathbf{r}')$ at $\mathbf{r}'$, (iv) propagated to $\mathbf{r}''$ and (v) scattered again by the potential $V(\mathbf{r}'')$ at $\mathbf{r}''$ *etc.* to yield a multiple-scattering formalism.

For multiple-electron atoms, multiple-particle systems, molecules and solid-state quantum systems, we can generate similar time-independent wavefunctions (eigenfunctions) Ψ_n by summing over all electron or particle momenta in a self-consistent manner, which is beyond the scope of this introduction. Common steps in standard texts include the Born–Oppenheimer approximation to decouple the motion of the nuclei from that of the electrons, antisymmetrization to ensure that the electron wavefunctions obey the Pauli exclusion principle for fermions *etc.* Following a standard phasor representation for the vector potential **A**, **E** and **B**, setting $\varphi = 0$ without loss of generality,

$$\begin{aligned}\mathbf{A} &= \sum_j \{\mathbf{A}_{j0}\exp[i(\omega_j t - \mathbf{k}\cdot\mathbf{r})] + \mathbf{A}_{j0}\exp[-i(\omega_j t - \mathbf{k}\cdot\mathbf{r})]\}, \\ \mathbf{E} &= \sum_j [2\omega\mathbf{A}_{j0}\sin(\omega_j t - \mathbf{k}_j\cdot\mathbf{r})] = \sum_j [\mathbf{E}_{j0}\sin(\omega_j t - \mathbf{k}_j\cdot\mathbf{r})], \\ \mathbf{B} &= \sum_j [2\mathbf{k}\times\mathbf{A}_{j0}\sin(\omega_j t - \mathbf{k}_j\cdot\mathbf{r})] = \sum_j [\mathbf{B}_{j0}\sin(\omega_j t - \mathbf{k}_j\cdot\mathbf{r})]. \end{aligned} \tag{52}$$

In more advanced operator quantum theory, we must quantize the electromagnetic fields (photons) and write the equations in terms of specific creation operators $\hat{a}_{\mathbf{k}}^{\dagger}$ and annihilation operators $\hat{a}_{\mathbf{k}}$ which define the allowed states as a finite sum of specific occupied modes of the field (*i.e.* a specific number of photons). In other words, the amplitude coefficients must be quantized multiples of the corresponding operators. See Loudon (2000), Bransden & Joachain (1983) and Sakurai (1994) for examples including the simple harmonic oscillator. The solution from quantum mechanics is

$$\begin{aligned}\mathbf{A}(\mathbf{r},t) &= \sum_{\mathbf{k}}\left(\frac{\hbar}{2\varepsilon_0 V\omega_k}\right)^{1/2}\boldsymbol{\varepsilon}_{\mathbf{k}}\{\hat{a}_{\mathbf{k}}\exp[i(\mathbf{k}\cdot\mathbf{r} - \omega_k t)] \\ &\quad + \hat{a}_{\mathbf{k}}^{\dagger}\exp[-i(\mathbf{k}\cdot\mathbf{r} - \omega_k t)]\}, \\ \mathbf{E}(\mathbf{r},t) &= \sum_{\mathbf{k}} i\left(\frac{\hbar\omega_k}{2\varepsilon_0 V}\right)^{1/2}\boldsymbol{\varepsilon}_{\mathbf{k}}\{\hat{a}_{\mathbf{k}}\exp[i(\mathbf{k}\cdot\mathbf{r} - \omega_k t)] \\ &\quad - \hat{a}_{\mathbf{k}}^{\dagger}\exp[-i(\mathbf{k}\cdot\mathbf{r} - \omega_k t)]\}, \\ \mathbf{B}(\mathbf{r},t) &= \sum_{\mathbf{k}} i\left(\frac{\hbar}{2\varepsilon_0 V\omega_k}\right)^{1/2}\mathbf{k}\times\boldsymbol{\varepsilon}_{\mathbf{k}}\{\hat{a}_{\mathbf{k}}\exp[i(\mathbf{k}\cdot\mathbf{r} - \omega_k t)] \\ &\quad - \hat{a}_{\mathbf{k}}^{\dagger}\exp[-i(\mathbf{k}\cdot\mathbf{r} - \omega_k t)]\}. \end{aligned} \tag{53}$$

Each mode of wavevector $\mathbf{k}$ and polarization $\boldsymbol{\varepsilon}_{\mathrm{k}}$ represents a quantum-mechanical harmonic oscillator whose creation and annihilation operators obey the standard commutation rules for bosons (light carries one unit of angular momentum and hence is a boson). V is the volume. Using the interaction picture Hamiltonian and standard time-dependent perturbation theory,

$$\begin{aligned}\mathbf{H}'(t) &= -\frac{e}{2m}(\mathbf{p}\cdot\mathbf{A} + \mathbf{A}\cdot\mathbf{p}) + \frac{e^2\mathbf{A}\cdot\mathbf{A}}{2m} + \frac{e\mathbf{S}\cdot\mathbf{B}}{m} \\ &\quad + \frac{e^2}{m(mc^2)}\mathbf{S}\cdot[\dot{\mathbf{A}}(\mathbf{r})\times\mathbf{A}(\mathbf{r})], \end{aligned} \tag{54}$$

where the last term arises from the expansion of the Dirac Hamiltonian and the term

$$\frac{e}{m(mc^2)}\mathbf{S}\cdot\mathbf{E}(\mathbf{r})\times[\mathbf{p} + e\mathbf{A}(\mathbf{r})].$$

Applying the rotating-wave approximation yields the transition rate: the probability per atom per unit time of a transition (absorption) between the many-electron wavefunction in an atom, molecule or quantum system from state $|i\rangle = \Psi_i$ to state $|j\rangle = \Psi_j$,

$$P_{ij} = |c_j(t)|^2/t = B_{ij}\rho(\omega_{ij}), \tag{55}$$

where P is the transition probability per unit time per photon energy density per unit bandwidth, B_{ij} is the Einstein B coefficient for (stimulated) absorption and $\rho(\omega_{ij})$ is the photon density of states. For nondegenerate levels $B_{ij} = B_{ji}$ follows directly from the hermiticity of the perturbation $\mathbf{H}'(t)$ (see, for example, Blume, 1994) and

$$|c_j(t)|^2 = |\langle j|\hat{\mathbf{H}}'|i\rangle|^2 A_0^2\frac{\sin^2[(\omega_{ji} - \omega)t/2]}{\hbar^2[(\omega_{ji} - \omega)/2]^2}. \tag{56}$$

For many sources, the incident photon distribution is broad; that is, $\rho(\omega)$ is a slowly varying function of ω. From the operator formalism, the time-dependent perturbation must be an operator $\hat{\mathbf{H}}'(t)$. Hence, integrating over a (narrow) range of angular frequencies around ω_{ij} leads to

$$\begin{aligned} P_{ij} &= |c_j(t)|^2/t = \frac{\pi}{\varepsilon_0\omega_{ij}^2\hbar^2}|\langle j|\hat{\mathbf{H}}'(t)|i\rangle|^2\rho(\omega_{ij}), \\ \hat{\mathbf{H}}'(t) &\simeq A_0\frac{e}{m}\Big(\boldsymbol{\varepsilon}_{\mathbf{k}}\cdot\mathbf{p}\exp(i\mathbf{k}\cdot\mathbf{r}) + i\mathbf{S}\cdot\mathbf{k}\times\boldsymbol{\varepsilon}_{\mathbf{k}}\exp(i\mathbf{k}\cdot\mathbf{r}) \\ &\quad + \frac{eA_0'}{2}\boldsymbol{\varepsilon}_{\mathbf{k}}'\cdot\boldsymbol{\varepsilon}_{\mathbf{k}}\exp[i(\mathbf{k} - \mathbf{k}')\cdot\mathbf{r}] \\ &\quad + \frac{eA_0'}{mc^2}\mathbf{S}\cdot\{[\boldsymbol{\varepsilon}_{\mathbf{k}'}\exp(-i\mathbf{k}'\cdot\mathbf{r})]\times[\boldsymbol{\varepsilon}_{\mathbf{k}}\exp(i\mathbf{k}\cdot\mathbf{r})]\}\Big). \end{aligned} \tag{57}$$

To deal with many electrons in an atom or a more complex quantum system, we would simply replace $\mathbf{p}\exp(i\mathbf{k}\cdot\mathbf{r})$ with $\sum_i \mathbf{p}_i\exp(i\mathbf{k}\cdot\mathbf{r}_i)$ for the sum of electron momenta and locations.

It has been mentioned earlier that in order to determine the physical state of a system it is necessary to interact with it using some kind of probe, in this case a photon. In moving to a quantum-mechanical formulation of the photon scattering process it is necessary to formulate a rule to describe the probability of transition between energy levels (from one eigenstate $|i\rangle$ to another eigenstate $\langle j|$) in a continuum when

the system is subjected to a weak perturbation. Fermi's golden rule is such a rule. In its simplified form it states that the transition probability $P_{ij} \simeq (2\pi/h)|\langle j|H'|i\rangle|^2\rho$, where ρ is the density of final states and H' is the matrix element of the perturbation linking $|i\rangle$ to $\langle j|$, as we have just discussed.

Sum rules in quantum mechanics are formulae which describe transitions between energy levels in which the sum of the transition strengths is expressed in a simple manner. Sum rules are used to describe many systems: atoms, molecules, assemblages of atoms and molecules, and so on. They are derived using general principles and are useful when the behaviour of individual energy levels is too complex to be described precisely using quantum theory. They use the Heisenberg terminology and algebraic structure. The transition probabilities of the overall transitions are related to the idea of the concept of oscillator strength which was introduced in Section 4. One such rule is the *Thomas–Reiche–Kuhn* rule. The oscillator strength for a transition from state $|i\rangle = |1\rangle$ to $\langle j| = \langle 2|$, f_{12}, is given by

$$f_{12} = \frac{4m_e}{\hbar^2}(E_2 - E_1)\sum|\langle 1m_1|R_p|2m_2\rangle|^2,$$

where the summation is over the spatial coordinates x, y, z; $R_p = \sum_i x_i$, where the summation is from $i = 1$ to $i = N$, $|n_i\rangle$ can be 1 or 2, and each of the n_i may have degenerate sublevels m_n.

Consider the Hamiltonian $H = (p^2/2m_e) + V(r)$, so the commutator $[H, x] = i\hbar p_x/m_e$. Then,

$$x_{nk} = -\frac{i\hbar}{m_e(E_1 - E_2)}(p_x)_{nk}.$$

Calculating the matrix elements for $[p_x, x]$ leads to

$$\langle n|[p_x, x]|k\rangle = \frac{e\hbar}{im_e}\sum_n|\langle n|p_x|k\rangle|^2/(E_n - E_k),$$

with the summation being over all k except $k = n$. Remembering that $[p_x, x] = i\hbar$, the expression for the sum rule is reached: $\sum_n f_{nk} = 1$, where $f_{nk} = (2/m_e)|\langle n|p_x|k\rangle|^2/(E_n - E_k)$.

In the current era, with the advent of ultrafast pulsed high-intensity X-ray sources, the complex time-dependencies including the assumptions of time-dependent perturbation theory can become important, measureable and observed. This is especially true with attosecond pump–probe experiments and with X-ray free-electron laser sources and interactions. In such cases, discussed in part later in this volume, and in part in Chantler (2024), these temporal dependencies can become important. The most direct and obvious impact of time-dependent perturbation theory is, however, the nature of transition probabilities and the observation of selection rules for atomic and quantum system transitions, as discussed next.

6. Quantum-mechanical basis of photon interaction: transition probabilities

Equations (54) and (57) generate and generalize to Fermi's golden rule (number 2), including up to second-order perturbation theory, with photon scattering wavevector $\mathbf{K} = \mathbf{k} - \mathbf{k}'$,

$$P_{ij} = |c_j(t)|^2/t = \frac{2\pi}{\hbar}\left|\langle j|\hat{\mathbf{H}}'(t)|i\rangle + \sum_k \frac{\langle j|\hat{\mathbf{H}}'(t)|k\rangle\langle k|\hat{\mathbf{H}}'(t)|i\rangle}{E_j - E_i - \hbar\omega}\right|^2 \times \delta(E_j - E_i - \hbar\omega),$$

$$\hat{\mathbf{H}}'(t) \simeq A_0\frac{e}{m}\sum_i\left[\boldsymbol{\varepsilon}_{\mathbf{k}}\cdot\mathbf{p}_i\exp(i\mathbf{k}\cdot\mathbf{r}_i) + i\mathbf{S}_i\cdot\mathbf{k}\times\boldsymbol{\varepsilon}_{\mathbf{k}}\exp(i\mathbf{k}\cdot\mathbf{r}_i) + \frac{eA_0'}{2}\exp(i\mathbf{K}\cdot\mathbf{r}_i)\left(\boldsymbol{\varepsilon}'_{\mathbf{k}}\cdot\boldsymbol{\varepsilon}_{\mathbf{k}} - i\frac{\hbar\omega}{mc^2}\mathbf{S}_i\cdot(\boldsymbol{\varepsilon}'_{\mathbf{k}}\times\boldsymbol{\varepsilon}_{\mathbf{k}})\right)\right]. \quad (58)$$

The Dirac delta function δ selects the photon density of states of the X-ray source distribution $\rho(\omega_{ij})$, which conserves energy. Fermi's golden rule implies that the transition probability is linear with (small) time intervals, yielding an exponential after integrating over finite times. The $\mathbf{A}\cdot\mathbf{A}$ or $(eA_0'/2)\boldsymbol{\varepsilon}'_{\mathbf{k}}\cdot\boldsymbol{\varepsilon}_{\mathbf{k}}$ term is the 'seagull' term. This represents first-order perturbation theory scattering of the field and corresponds to the Thomson term, Thomson scattering and also nonresonant inelastic scattering (NIXS) (Sakurai, 1967). It is typically seen as $\mathbf{A}^*\cdot\mathbf{A}$ or $\hat{a}_{\mathbf{k}}\cdot\hat{a}^{\dagger}_{\mathbf{k}}$ or $\hat{a}'_{\mathbf{k}}\cdot\hat{a}^{\dagger}_{\mathbf{k}}$ terms, *i.e.* as absorption and emission operators. If one uses relativistic theory, this interpretation is clarified.

If we consider a transition between two states as implied in the first-order term of Fermi's golden rule, with a radiation intensity

$$I = \frac{c\varepsilon_0}{2}|E|^2 = \frac{4c\omega^2A_0^2\varepsilon_0}{2}$$

(in W m^{-2}) then the cross section (in barns per atom) corresponds to (Joly & Grenier, 2016; Kas *et al.*, 2016; Mobilio, 2015; Bertoni, 2015)

$$\sigma_{ij} = \frac{\hbar\omega P_{ij}}{I} = \frac{4\pi}{4c\varepsilon_0\omega A_0^2}|\langle j|\hat{\mathbf{H}}'(t)|i\rangle|^2\delta(E_j - E_i - \hbar\omega). \quad (59)$$

If the final state is a continuum state then

$$\frac{d^2\sigma_{ij}}{dE'_e d\Omega_e} = \frac{\hbar\omega P_{ij}}{I} = \frac{4\pi}{4c\varepsilon_0\omega A_0^2}|\langle j, e'|\hat{\mathbf{H}}'(t)|i\rangle|^2\delta(E_j + E'_e - E_i - \hbar\omega), \quad (60)$$

where the total cross section would then integrate over the resonance continuum electron energy E'_e and the electron scattering vector to yield the total process cross section σ_{ij}.

If we consider a resonant inelastic scattering process to a final bound state, then the second-order term is critical and

$$\frac{d^2\sigma_{ij}}{d\omega' d\Omega} = \frac{\hbar\omega P_{ij}}{I} \quad (61)$$

indicates the vector direction of the scattered photon of energy ω', and the integral over the resonance photon energy and over the photon scattering vector will yield the total process cross section σ_{ij}. Similarly, if the final state is a continuum state then

$$\frac{d^4\sigma_{ij}}{d\omega' d\Omega dE'_e d\Omega_e} = \frac{\hbar\omega P_{ij}}{I}, \quad (62)$$

where the total cross section would then integrate over the resonance photon energy, the photon scattering vector, the resonance continuum electron energy E'_e and the electron scattering vector to yield the total process cross section σ_{ij}.

As an illustration, the mass absorption coefficient in $cm^2\ g^{-1}$ is related to the photoelectric cross section in barns per atom by

$$\left[\frac{\mu}{\rho}\right]_{PE} = \frac{\sigma_{PE}}{uA}, \tag{63}$$

where u is the atomic mass unit and A is the relative atomic mass.

We can perform a Taylor series expansion of the exponential of equation (58) or (59) (for a particular electron or orbital) to yield multipole operators (electric dipole radiation $E1$, $\hat{o}_{E1}$, electric quadrupole radiation $E2$, $\hat{o}_{E2}$, magnetic dipole radiation $M1$, $\hat{o}_{M1}$, electric octopole radiation $E3$, $\hat{o}_{E3}$ ...) and define selection rules for transition probabilities,

$$\begin{aligned}
\left\langle j\left|\frac{\hat{\mathbf{H}}'(t)}{A_0}\right|i\right\rangle &= i\frac{e}{\hbar}(E_j - E_i)\langle j|\hat{o}|i\rangle;\\
\hat{o} &= \hat{o}_{E1} + \hat{o}_{E2} + \hat{o}_{M1} + \hat{o}_{E3} + \ldots;\\
\hat{o}_{E1} &= \boldsymbol{\varepsilon}_{\mathbf{k}}\cdot\mathbf{r};\\
\hat{o}_{E2} &= \frac{i}{2}(\boldsymbol{\varepsilon}_{\mathbf{k}}\cdot\mathbf{r})(\mathbf{k}\cdot\mathbf{r});\\
\hat{o}_{M1} &= \frac{\hbar}{2m_e(E_j - E_i)}(\mathbf{k}\times\boldsymbol{\varepsilon}_{\mathbf{k}})\cdot(\mathbf{L} + 2\mathbf{S});\\
\hat{o}_{E3} &= -\frac{1}{6}(\boldsymbol{\varepsilon}_{\mathbf{k}}\cdot\mathbf{r})(\mathbf{k}\cdot\mathbf{r})^2;\ldots
\end{aligned} \tag{64}$$

These operators define the expected relative magnitudes and symmetries of allowed transitions, including the polarization vector coupling. In cylindrical coordinates the electric field vector can be defined as a sum of three linear polarizations or in general as any linear combination of the three polarizations

$$\boldsymbol{\varepsilon}_{\mathbf{k}} = \hat{\mathbf{z}};\quad \boldsymbol{\varepsilon}_{\mathbf{k},+} = \frac{-1}{2^{1/2}}(\hat{\mathbf{x}} + i\hat{\mathbf{y}});\quad \boldsymbol{\varepsilon}_{\mathbf{k},-} = \frac{1}{2^{1/2}}(\hat{\mathbf{x}} - i\hat{\mathbf{y}}). \tag{65}$$

This represents plane- or π-polarized radiation and right-handed and left-handed circularly polarized radiation σ_+ and σ_-, respectively. For X-ray absorption edges the $E1$ operator is dominant, while above about 4.5 keV the $E2$ operator can be significant and follows different selection rules; $E3$ and $M1$ channels are difficult to detect in absorption spectra but are easily identified in medium- to high-Z materials in discrete bound–bound transitions (such as in dominant transitions in few-electron X-ray spectra) across the X-ray regime.

Consider a transition from an electronic wavefunction with quantum numbers $|\mathrm{i}\rangle = |l_i, m_{li}, m_{si}, \ldots, L, S, J, M_J\pi\rangle$ to a final state $|\mathrm{f}\rangle = |l'_i, m'_{li}, m'_{si}, \ldots, L', S', J', M'_J\pi'\rangle$. The selection rules for electric dipole radiation include the following.

(i) *Parity* π. The electric dipole operator only connects states of opposite parity. The radial operator is odd in parity, so any wavefunction with a defined parity must change to the opposite parity. From parity considerations in Legendre polynomials, we can state Δl_i = odd (strictly). For $l = 0$, or an s-state, parity is even; for $l = 1$, or a p-state, parity is odd; for l = odd, parity is odd.

(ii) *Magnetic orbital angular momentum quantum number* m_l. The separability of the radial and angular dependence of the wavefunctions implies selection rules for changes in m_l (the z-projection magnetic quantum number). Hence, $m'_l - m_l = 0, +1$ or -1. For example, if $\boldsymbol{\varepsilon}_{\mathbf{k}} = \hat{\mathbf{z}}$ then $\Delta m_l = 0$. Hence, this π-polarized radiation has an electric dipole selection rule of $\Delta m_l = 0$. Similarly, $\sigma_{+/-}$ circularly polarized radiation requires $\Delta m_l = \mp 1$, respectively.

(iii) l_i and s_i. In low-energy or LS (Russell–Saunders) coupling, which is suitable for low-Z atoms, the individual quantum numbers l_i and s_i for each electron sum vectorially to a total L (orbital angular momentum quantum number) and a total S (spin angular momentum quantum number) for the atomic quantum system, which then sum to a total J (the total angular momentum quantum number). The 'good' quantum numbers are L, S, J and M_J in the nonrelativistic atomic system before coupling to nuclear, molecular or solid-state wavefunctions.

In the case of magnetic dipole radiation $M1$, whether the perturbing Hamiltonian does or does not include the spin term makes a major difference to the selection rules. Including the spin term in the Hamiltonian H', and using Cartesian coordinates for polarizations, the angular spherical harmonic integrals yield

$$\begin{aligned}
&\langle l'_i m'_{li} m'_{si} \ldots |L_x + g_s S_x| l_i m_{li} m_{si} \ldots\rangle =\\
&\quad \hbar\left\{\frac{1}{2}[l'_i(l'_i-1) - m'_{li}(m'_{li}-1)]^{1/2}\delta_{m_{li},m'_{li}}\right.\\
&\quad +\frac{1}{2}[l'_i(l'_i-1) - m'_{li}(m'_{li}+1)]^{1/2}\delta_{m_{li},m'_{li}+1}\delta_{m_{si},m'_{si}}\\
&\quad \left.+\frac{g_s}{2}\delta_{m_{li},m'_{li}}\delta_{m_{si},-m'_{si}}\right\}\delta_{l_i,l'_i}\\
&\langle l'_i m'_{li} m'_{si} \ldots |L_y + g_s S_y| l_i m_{li} m_{si} \ldots\rangle =\\
&\quad i\hbar\left\{\frac{1}{2}[l'_i(l'_i-1) - m'_{li}(m'_{li}-1)]^{1/2}\delta_{m_{li},m'_{li}-1}\right.\\
&\quad -\frac{1}{2}[l'_i(l'_i-1) - m'_{li}(m'_{li}+1)]^{1/2}\delta_{m_{li},m'_{li}+1}\delta_{m_{si},m'_{si}}\\
&\quad \left.+(-1)^{m'_{si}+3/2}\frac{g_s}{2}\delta_{m_{li},m'_{li}}\delta_{m_{si},-m'_{si}}\right\}\delta_{l_i,l'_i}\\
&\langle l'_i m'_{li} m'_{si} \ldots |L_z + g_s S_z| l_i m_{li} m_{si} \ldots\rangle =\\
&\quad \hbar\left\{\langle[m'_{li} + (-1)^{m'_{si}+3/2}\frac{g_s}{2}\rangle]\delta_{m_{li},m'_{li}}\delta_{m_{si},m'_{si}}\right\}\delta_{l_i,l'_i}.
\end{aligned} \tag{66}$$

Hence, the selection rule from orbital angular momentum $\Delta S = 0$ becomes, naturally, $\Delta S = 0, \pm 1$ upon inclusion of the spin interaction, and in general the angular integrals yields selection rules as in Table 1.

Incidentally, the dominant decay mode for excited states is often radiationless Auger transitions, including Coster–Kronig transitions. These have selection rules as listed.

Therefore, for an s-electron ionization (the K, L_1 or M_1 edges), electric dipole radiation $E1$ probes p orbitals, electric quadrupole radiation $E2$ probes d orbitals, magnetic dipole radiation $M1$ probes s orbitals and electric octopole radiation

Table 1
Selection rules for multipole transitions.

Allowed transitions	Electric dipole ($E1$)	Magnetic dipole ($M1$)	Electric quadrupole ($E2$)	Magnetic quadrupole ($M2$)	Electric octopole ($E3$)	Magnetic octopole ($M3$)	Auger
Rigorous rules	$\Delta J = 0, \pm 1$ ($J = 0 \not\rightarrow 0$) $\Delta M_J = 0, \pm 1$ ($\Delta M_J = 0 \not\rightarrow 0$ if $\Delta J = 0$)		$\Delta J = 0, \pm 1, \pm 2$ ($J = 0 \not\rightarrow 0, 1; \frac{1}{2} \not\rightarrow \frac{1}{2}$) $\Delta M_J = 0, \pm 1, \pm 2$		$\Delta J = 0, \pm 1, \pm 2, \pm 3$ ($0 \not\rightarrow 0, 1, 2; \frac{1}{2} \not\rightarrow \frac{1}{2}, \frac{3}{2}; 1 \not\rightarrow 1$) $\Delta M_J = 0, \pm 1, \pm 2, \pm 3$		$\Delta J = 0$ $\Delta M_J = 0$
Parity	$\pi_f = -\pi_i$		$\pi_f = \pi_i$		$\pi_f = -\pi_i$	$\pi_f = \pi_i$	$\pi_f = \pi_i$
LS coupling	One electron jump $\Delta l_i = \pm 1$ $\Delta m_{li} = 0, \pm 1$ $\Delta s_i = 0$ $\Delta S = 0$ $\Delta L = 0, \pm 1$ ($L = 0 \not\rightarrow 0$)	No electron jump $\Delta l_i = 0$, $\Delta n = 0$ $\Delta m_{li} = 0$ $\Delta s_i = 0, \pm 1$ $\Delta S = 0, \pm 1$ $\Delta L = 0$ $\Delta J = \pm 1$	No or one jump $\Delta l_i = 0, \pm 2$ $\Delta m_{li} = 0, \pm 1, \pm 2$ $\Delta s_i = 0$ $\Delta S = 0$ $\Delta L = 0, \pm 1, \pm 2$	One jump $\Delta l_i = \pm 1$ $\Delta m_{li} = \pm 1$ $\Delta s_i = 0$ $\Delta S = 0$ $\Delta L = \pm 1$ ($L = 0 \not\rightarrow 0, 1$)	One jump $\Delta l_i = \pm 1, \pm 3$ $\Delta m_{li} = 0, \pm 1, \pm 2, \pm 3$ $\Delta s_i = 0$ $\Delta S = 0$ $\Delta L = 0, \pm 1, \pm 2, \pm 3$ ($L = 0 \not\rightarrow 0, 1, 2; 1 \not\rightarrow 1$)	One jump $\Delta l_i = 0, \pm 2$ $\Delta m_{li} = 0, \pm 2$ $\Delta s_i = 0$ $\Delta S = 0$ $\Delta L = 0, \pm 2$	No jump $\Delta l_i = 0$ $\Delta m_{li} = 0$ $\Delta s_i = 0$ $\Delta S = 0$ $\Delta L = 0$
Intermediate coupling	If $\Delta S = 0$, $\Delta L = 0, \pm 1$ ($L = 0 \not\rightarrow 0$)	If $\Delta S = 0$, $\Delta L = 0$	If $\Delta S = 0$, $\Delta L = 0, \pm 1, \pm 2$ ($L = 0 \not\rightarrow 0, 1$)		If $\Delta S = 0$, $\Delta L = 0, \pm 1, \pm 2, \pm 3$ ($L = 0 \not\rightarrow 0, 1, 2; 1 \not\rightarrow 1$)		
Intermediate coupling	If $\Delta S = \pm 1$, $\Delta L = 0, \pm 1, \pm 2$		If $\Delta S = \pm 1$, $\Delta L = 0, \pm 1, \pm 2, \pm 3$ ($L = 0 \not\rightarrow 0$)	If $\Delta S = \pm 1$, $\Delta L = 0, \pm 1$ ($L = 0 \not\rightarrow 0$)	If $\Delta S = \pm 1$, $\Delta L = 0, \pm 1, \pm 2, \pm 3$, ± 4 ($L = 0 \not\rightarrow 0, 1$)	If $\Delta S = \pm 1$, $\Delta L = 0, \pm 1, \pm 2$ ($L = 0 \not\rightarrow 0$)	

$E3$ probes p and f orbitals. For ionization from a p shell ($L_{2,3}$ and $M_{2,3}$ edges), electric dipole radiation $E1$ probes the s and d orbitals (usually dominated by the d-orbital interaction) while $E2$ radiation probes the p and f orbitals.

For higher-Z systems, inner-shell processes and general X-ray energies, LS coupling breaks down and intermediate or jj coupling become the clearer definition of well defined quantum numbers and hence selection rules (Bransden & Joachain, 1983). However, the general problem is therefore an intermediate coupling problem where an eigenstate is defined by a sum of configuration state functions, which represents a more complex system but is necessary for high-accuracy computations (Grant, 1973; Jönsson *et al.*, 2013). Similarly, a fully relativistic wavefunction requires a yet different parametrization (Grant, 2007; see also Fujikawa, 2024).

The dominant $\mathbf{A} \cdot \mathbf{p}$ term gives X-ray absorption in the lowest order, and XAFS in higher orders, and resonant elastic X-ray scattering (REXS, X-ray diffraction) and resonant inelastic X-ray scattering (RIXS) in the second and higher orders. The spin term and spin–orbit term are crucial for $M1$ magnetic dipole radiation and transitions, and are also crucial for magnetic scattering, and the final term from the higher-order reduction of the Dirac equation is important for magnetic scattering and magnetic systems, and also arises as a first-order perturbation theory; for a 10 keV X-ray, for example, it is approximately $\hbar\omega/mc^2 \simeq 0.02$ times the Thompson term. The magnetic X-ray scattering cross section vanishes at forward momentum ($\mathbf{q} = 0$) and does not contribute to absorption (Vettier, 1994).

The transition probabilities thus enunciated allow any manner of inelastic scattering processes including photoabsorption and elastic scattering as a limiting form, so that the processes discussed qualitatively at the beginning of this chapter can now be explored quantum-mechanically as scattering processes, as follows.

7. Scattering

Thomson (1906) derived the classical result for the total scattering (integrated over angles) of an X-ray by free electrons

$$\sigma_T = \frac{8\pi r_e^2}{3}, \tag{67}$$

where $r_e = e^2/(m_e c^2) \simeq 2.82 \times 10^{-15}$ m is the classical electron radius, the transition amplitude $A^R = f(\mathbf{q}, \omega)$ and the terms multiplying f are the Thomson cross section. The corresponding Thomson differential cross section (Thomson & Thomson, 1933) for the scattering of unpolarized radiation by a classical free electron, also not observing the polarization of the scattered radiation, is

$$\frac{d\sigma_T}{d\Omega} = \frac{r_e^2}{2}(1 + \cos^2\theta), \tag{68}$$

where θ is the scattering angle through which the wavevector of the radiation has changed (for diffraction, $\Theta_B = \theta/2$). Compton (1923*b*) recognized that the scattered energy from a free electron would change:

$$\hbar\omega' = \frac{\hbar\omega}{1 + \dfrac{\hbar\omega}{m_e c^2}(1 - \cos\theta)}. \tag{69}$$

The differential cross section for Compton scattering from a free electron, averaged over initial and summed over final photon and electron polarizations, is given by the Klein–Nishina formula (Klein & Nishina, 1929) from lowest-order relativistic quantum mechanics,

$$\frac{d\sigma_{KN}}{d\Omega} = \frac{r_e^2}{2}\left(\frac{\omega'}{\omega}\right)^2\left(\frac{\omega'}{\omega} + \frac{\omega}{\omega'} - \sin^2\theta\right), \tag{70}$$

which reduces to the Thomson differential cross section in the limit $\omega' \rightarrow \omega$ where the scattered photon frequency becomes that of the incident photon and the cross section becomes that of an elastic system. Where a second-order process such as scattering is involved, the differential cross section $d\Sigma/d\Omega$ can be integrated over the 4π range for the vector of the outgoing photon or electron to yield the total cross section for that process. The low-energy expansion of the Klein–Nishina formula for Compton scattering from a free electron (Jackson, 1975; Berestetskii *et al.*, 1982) is given by

$$\sigma_{\rm KN} = \pi r_{\rm e}^2 \int_{-1}^{1} \frac{1+\cos^2\theta + \dfrac{k^2(1-\cos\theta)^2}{1+k(1-\cos\theta)}}{[1+k(1-\cos\theta)]^2}\,{\rm d}(\cos\theta), \quad k = \frac{\hbar\omega}{m_{\rm e}c^2}$$
$$\simeq \sigma_T\left(1 - \frac{2\hbar\omega}{m_{\rm e}c^2} + \ldots\right), \quad \hbar\omega \ll m_{\rm e}c^2. \tag{71}$$

7.1. Polarizations in scattering

For Rayleigh (elastic photon) scattering, assuming that the atom is not polarized or aligned, there are two independent scattering amplitudes for the incident and scattered polarization and wavevector, corresponding to scalars

$$\frac{{\rm d}\sigma_{\rm R}}{{\rm d}\Omega} = \frac{r_{\rm e}^2}{2}|A|^2,$$
$$A = \hat{\varepsilon}\cdot\hat{\varepsilon}'^{*}M_1(\mathbf{k}\cdot\mathbf{k}') + \hat{\varepsilon}\cdot\hat{k}'\hat{\varepsilon}'^{*}\cdot\hat{k}M_2(\mathbf{k}\cdot\mathbf{k}'),$$
$$\hat{k} = \frac{\mathbf{k}}{|\mathbf{k}|}, \tag{72}$$

where these are most readily resolved in polarizations in the plane of scattering $\hat{\varepsilon}_\parallel$ and out of the plane of scattering $\hat{\varepsilon}_\perp$. Then,

$$\hat{\varepsilon}_\perp\cdot\hat{\varepsilon}'^{*}_\perp = 1, \quad \hat{\varepsilon}_\parallel\cdot\hat{\varepsilon}'^{*}_\parallel = \cos\theta,$$
$$\hat{\varepsilon}_\perp\cdot\hat{k}'^{*} = \hat{k}\cdot\hat{\varepsilon}'^{*}_\perp = 0, \quad \hat{\varepsilon}_\parallel\cdot\hat{k}'^{*} = -\hat{k}\cdot\hat{\varepsilon}'^{*}_\parallel = \sin\theta,$$
$$A = \hat{\varepsilon}_\parallel\cdot\hat{\varepsilon}'^{*}_\parallel[M_1(\mathbf{k}\cdot\mathbf{k}')\cos\theta - M_2(\mathbf{k}\cdot\mathbf{k}')\sin^2\theta] + \hat{\varepsilon}_\perp\cdot\hat{\varepsilon}'^{*}_\perp M_1(\mathbf{k}\cdot\mathbf{k}')$$
$$= \hat{\varepsilon}_\parallel\cdot\hat{\varepsilon}'^{*}_\parallel A_\parallel + \hat{\varepsilon}\perp\cdot\hat{\varepsilon}'^{*}_\perp A_\perp. \tag{73}$$

The nature of the experiment becomes important in determining the relevant observables and hence the relevant integrals. In general, whenever an experimental (or theoretical) system does not fully specify the incident photon polarization, the target orientation and alignment, and where the outgoing channels may include photoelectrons *etc.*, the density-matrix formalism is able to represent the observables by statistical sum or integration (Åberg & Tulkki, 1985). In the limit of undefined orientation and alignment, the cross section for scattering photons polarized perpendicular to the plane of scattering becomes

$$\frac{{\rm d}\sigma_{\rm R\perp}}{{\rm d}\Omega} = |A_\perp|^2, \tag{74}$$

with the cross section for scattering photons polarized parallel to the plane of scattering being

$$\frac{{\rm d}\sigma_{\rm R\parallel}}{{\rm d}\Omega} = |A_\parallel|^2, \tag{75}$$

so that the cross section for unpolarized photons, averaged over incident-photon polarizations and summed over scattered-photon polarizations, is given as

$$\frac{{\rm d}\sigma_{\rm R}}{{\rm d}\Omega} = \frac{1}{2}(|A_\perp|^2 + |A_\parallel|^2). \tag{76}$$

For Thomson scattering $A_\perp^{\rm T} = -r_{\rm e}$, $A_\parallel^{\rm T} = -r_{\rm e}\cos\theta$. For the high-energy limit, $A_\perp^{\rm R} = -r_{\rm e}N_{\rm e}$, $A_\parallel^{\rm R} = -r_{\rm e}N_{\rm e}\cos\theta$, where $N_{\rm e}$ is the number of electrons per atom. For a neutral atom $N_{\rm e} = Z$; however, the (atomic) electrons cannot be treated as point charges and instead scatter as a form factor which can follow the form-factor approximation (James, 1962) $A_\perp^{\rm R} = -r_{\rm e}f(\mathbf{q},\omega)$, $A_\parallel^{\rm R} = -r_{\rm e}f(\mathbf{q},\omega)\cos\theta$, which approaches $N_{\rm e}$ for low momentum transfer and approaches zero for high momentum transfer.

In the form-factor approximation, the differential scattering cross section for elastic Rayleigh scattering, for unpolarized photons, averaged over final polarization, is therefore given by

$$\frac{{\rm d}\sigma_{\rm R}}{{\rm d}\Omega} = \frac{r_{\rm e}^2}{2}(1+\cos^2\theta)|f(\mathbf{q},\omega)|^2 = \frac{{\rm d}\sigma_{\rm T}}{{\rm d}\Omega}|f(\mathbf{q},\omega)|^2, \tag{77}$$

where the form factor, equation (38), is the Fourier transform of the electron density.

Some confusion exists in the literature in definitions of the form-factor approximation. The simplest is that

$$f\left(\mathbf{q} = \mathbf{k}_{\rm f} - \mathbf{k}_{\rm i} = \frac{2\omega\sin(\theta/2)}{c}, \omega\right) = \int \rho(r)\exp[i(\mathbf{k}_{\rm f} - \mathbf{k}_{\rm i})\cdot\mathbf{r}]\,{\rm d}V,$$

the *first-order form-factor approximation*, which is known to be poor and fails to represent any resonances and absorption edges. Usually there are limitations of the form-factor approximation at high momentum transfers and high energies, where $\hbar q \geq 0.2mc$ or where the atomic inner-shell electron has $(v/c)^2 \simeq \frac{1}{2}(Z\alpha/n)^2$ becoming large. In an intermediate regime, the *modified form-factor formalism*, mff, which includes a next-order correction for the (atomic) binding potential, can improve the accuracy of predictions. This has been used extensively in developments involving the **S**-matrix formalism, with some encouraging results in comparisons of measurements on medium- and high-Z targets with theory (Muckenheim & Schumacher, 1980; Kissell & Pratt, 1985; Kane *et al.*, 1986; Crasemann, 1996). Unfortunately, the more complex versions of the **S**-matrix formalism remain highly computational and no generic tables have been produced on this basis. Additionally, they are limited by the accuracy of the mff.

The greatest improvement is made by explicitly including the anomalous scattering factors, allowing high-accuracy computations for binding: the *complex form-factor approximation*, cff (Chantler, 1994, 2000). These are also represented in *International Tables for Crystallography Volume C* (Chantler & Creagh, 2024). The **q**-dependence of the anomalous scattering factors, both real and imaginary, remains a major question because the predictions are based around the forward scattering angle (equation 40). To first order, it appears that the expansion $f(\mathbf{q},\omega) = f_0(\mathbf{q}) + f'(\omega) + if''(\omega)$ is useful, where f_0 is defined by the usual (first-order) atomic form factor. The additional anomalous scattering factors arise directly from the second-order perturbation theory expansion and provide the absorption edges and resonant scattering. Notice that when the anomalous scattering is included the form factor is complex, with the real component representing Rayleigh scattering and the imaginary component representing absorption from each of the elastic scattering processes. Additionally, the quality of the result depends critically upon the quality of the quantum-mechanical wavefunctions, eigenvalues and the software used to generate these.

Tabulations of atomic form factors obtained using relativistic theory and advanced quantum mechanics are available, although they do not usually present results for individual shells or subshells (Chantler, 1995, 2000; Creagh, 1999). These typically depend upon a simplification of the most advanced atomic codes using a relativistic but density-functional theory (DFT) approximation rather than a fully relativistic Dirac–Hartree–Fock (DHF) approach to the computations (Grant, 2007; Chantler *et al.*, 2010; Pham *et al.*, 2016). The latest version of *International Tables for Crystallography Volume C* includes extensive tables for X-ray laboratory sources *etc.* (Chantler & Creagh, 2024) and also presents a detailed summary of the current agreement of the latest computations with experiment. In general, this is the state of the art for comprehensive predictions.

Significant developments in the understanding of these have been made with the **S**-matrix formalism, typically within the modified form-factor formalism, and with attempts at full relativistic matrix-element calculations.

7.2. Nuclear Thomson scattering

For a point nucleus the nuclear Thomson amplitude is $A_{\perp}^{\rm NT} = -r_{\rm e}Z^2(m_{\rm e}/M)$, $A_{\parallel}^{\rm NT} = A_{\perp}^{\rm NT}\cos\theta$; with the finite nuclear size included the amplitude is approximately

$$A_{\perp}^{\rm NT} = -r_{\rm e}Z^2\frac{m_{\rm e}}{M}\left(1-\frac{\omega^2}{3c^2}\langle r_{\rm N}^2\rangle\right).$$

This in turn can be well approximated by the Fermi model (Lowe *et al.*, 2013). In areas where both Rayleigh and nuclear Thompson scattering are observable, for unpolarized photons, the elastic scattering cross section is

$$\frac{{\rm d}\sigma_{\rm R}}{{\rm d}\Omega} = \frac{r_{\rm e}^2}{2}(1+\cos^2\theta)\left|f(\mathbf{q},\omega)+\frac{A_{\perp}^{\rm NT}}{r_{\rm e}}\right|^2 = \frac{{\rm d}\sigma_{\rm T}}{{\rm d}\Omega}\left|f(\mathbf{q},\omega)+\frac{A_{\perp}^{\rm NT}}{r_{\rm e}}\right|^2. \tag{78}$$

A few measurements have confirmed the preceding predictions with $A^{\rm NT} \simeq O[Z^2(m_{\rm e}/M)]$ (Kissell & Pratt, 1985; Ericson & Hüfner, 1973; Wright & Debevec, 1982).

7.3. Delbrück scattering

The imaginary part of the amplitude for Delbrück scattering is the absorptive process for pair production and is zero below $\hbar\omega < 2m_{\rm e}c^2 = 1.022$ MeV. The real component is a dispersion form corresponding to the same vacuum polarization and is ergo a nonlinear process of quantum electrodynamics (QED) for which there is no classical analogue. In principle, the real component is observable below ∼1 MeV for high-Z neutral systems such as uranium but is unimportant below 500 keV. Between 1 and ∼4 MeV strong interference can occur between the contributions of Rayleigh, nuclear Thomson and Delbrück scattering. Experiments (Rullhusen *et al.*, 1983) suggest that calculations using the lowest-order Born approximation might be accurate to a few percent for $Z < 60$.

The effect of these lowest-order QED processes, including the self-energy and vacuum polarization, are observable at room temperature and for all atomic numbers in high-accuracy experiments, especially with medium-Z atoms at the 10^{-5} or 10–20 parts per million level for X-ray energies and Lyman spectra.

7.4. Giant dipole resonances (GDR) and the elastic nuclear resonance cross section

For photon energies above 1 MeV, the complex nuclear structure allows nuclear resonances and in particular the giant dipole resonance. The photonuclear absorption cross section for the giant dipole (nuclear) resonance can be represented by a fit of two Lorentzian lineshapes. $A^{\rm NR}$ is purely real for energies below the (γ, n) threshold (for example ∼7.4 MeV for ^{208}Pb). Above the onset of the GDR, the nuclear structure and resonances become more complex (Hayward, 1993). Above ∼4 MeV, the GDR and $A^{\rm NR}$ dominate over the elastic cross sections; although in regions free of resonances the Delbrück scattering is able to once more be significant and observable. Normal synchrotron beamlines have maximum energies well below 100 keV, so the last two elastic and absorptive processes can be neglected, yet specialized experiments and facilities do access these higher energy regions. At low angles (forward scattering) the phases of Rayleigh and nuclear Thomson scattering ($A^{\rm R}$, $A^{\rm NT}$) are both negative, while the phases of Delbrück and nuclear resonance scattering are positive.

7.5. Inelastic scattering and fluorescence

In presenting the discussion of complex elastic scattering amplitudes, we have also explicitly discussed the photoabsorption amplitudes and cross sections. Following equations (43), (46), (49) and (51) for the development of perturbation theory expansions and equations (58), (61) and (62) for the perturbing time-dependent Hamiltonian, we have the core equations for inelastic scattering. To lowest order (semi-classically), and in sympathy with the derivation of the Klein–Nishina cross section, we have

$$\frac{{\rm d}^2\sigma_{ij}}{{\rm d}\omega'{\rm d}\Omega} = \frac{\hbar\omega P_{ij}}{I} = \frac{\pi}{c\varepsilon_0\omega A_0^2}\left|\langle j|\hat{\mathbf{H}}'(t)|i\rangle\right|^2\delta(E_j-E_i-\hbar\omega),$$
$$\hat{\mathbf{H}}'(t) \simeq A_0\frac{e}{m}\sum_i[\boldsymbol{\varepsilon}_{\mathbf{k}}\cdot\mathbf{p}_i\exp(i\mathbf{k}\cdot\mathbf{r}_i)+i\mathbf{S}\cdot\mathbf{k}\times\boldsymbol{\varepsilon}_{\mathbf{k}}\exp(i\mathbf{k}\cdot\mathbf{r}_i)]. \tag{79}$$

Fluorescent scattering, especially as a measurement type for X-ray absorption spectroscopy, is discussed in Chantler (2024) and elsewhere. In all such secondary processes, the timing structure of the experiment and detection becomes important in estimating the information content obtained.

In elastic scattering, $j = i$, $E_j = E_i + \hbar\omega' = E_i + \hbar\omega$ and $\rho(\mathbf{r}) = \Psi_n^*\sum_j\exp(-i\mathbf{k}\cdot\mathbf{r})\Psi_n$, so this is equivalent to our earlier $A_{\perp}^R = -r_{\rm e}f(\mathbf{q},\omega)$, $A_{\parallel}^{\rm R} = -r_{\rm e}f(\mathbf{q},\omega)\cos\theta$ and equation (77).

By contrast, for inelastic scattering to the same order, $\hbar\omega' = \hbar\omega + E_i - E_j$ and

$$\frac{\mathrm{d}^2\sigma_{ij}}{\mathrm{d}\omega'\mathrm{d}\Omega} = \frac{\pi}{c\varepsilon_0\omega A_0^2}\sum_{j\neq i}\frac{\omega'}{\omega}\left|\left\langle j\left|\sum_r \exp(-i\mathbf{q}\cdot\mathbf{r})\right|i\right\rangle\right|^2 \times \delta(E_j + \hbar\omega' - E_i - \hbar\omega) \quad (80)$$

and is the Compton cross section. At high energies $\omega' \simeq \omega$ and we note that

$$\sum_{j\neq i}\left|\left\langle j\left|\sum_r \exp(-i\mathbf{q}\cdot\mathbf{r})\right|i\right\rangle\right|^2 = N_\mathrm{e} - \sum_i\left|\left\langle i\left|\sum_r \exp(-i\mathbf{q}\cdot\mathbf{r})\right|i\right\rangle\right|^2, \quad (81)$$

where the number of electrons per atom $N_\mathrm{e} = Z$ in a neutral atom. Hence, at the same order of accuracy as the form-factor formalism, one can define an inelastic scattering factor $S(\mathbf{q}, \omega) = N_\mathrm{e} - |f(\mathbf{q}, \omega)|^2$ or $S(\mathbf{q}, \omega) = \sum_j |\langle j|\sum_r \exp(-\pi\mathbf{q}\cdot\mathbf{r})|i\rangle|^2 - |f(\mathbf{q}, \omega)|^2$. The formula for inelastic Compton scattering can then be generalized from the Klein–Nishina cross section as

$$\sigma_\mathrm{C} = \pi r_\mathrm{e}^2\int_{-1}^{1}\frac{1+\cos^2\theta + \dfrac{k^2(1-\cos\theta)^2}{1+k(1-\cos\theta)}}{[1+k(1-\cos\theta)]^2}\mathbf{S}(\mathbf{q}, Z)\,\mathrm{d}(\cos\theta),$$
$$k = \frac{\hbar\omega}{m_\mathrm{e}c^2}. \quad (82)$$

A general discussion of polarization dependence, the tensorial dependence of the lowest-order and higher order contributions, especially for inelastic scattering processes, is given elsewhere in this volume (Paolasini & Di Matteo, 2024; Šipr, 2024; van der Laan, 2024; van der Laan & Figueroa, 2024; Glatzel *et al.*, 2024) and in the wider literature (Åberg & Tulkki, 1985; Pratt *et al.*, 1994; Blume, 1994). For the angular dependence of elastic processes Figs. 5, 6, 9, 10 and 11 of Kissell & Pratt (1985) are particularly commended, and Fig. 2 of Åberg & Tulkki (1985) for elastic, inelastic and fluorescent peaks as a function of energy (incident, emission) and angle. Some authors distinguish inelastic 'Raman scattering' representing lower energy bound–bound excitations or threshold interactions near the absorption edge, perhaps by distinction from inelastic 'Compton scattering' from bound systems. In general these processes tend to overlap and are therefore nontrivial to separate, depending perhaps mainly on the inner-shell versus outer-shell excitation or ionization. In the high-energy limit, the photoelectron emission from photoabsorption is followed by a relaxation of the inner-shell hole in a second step, with almost no angular dependence; this may be by Auger electron emission or by X-ray fluorescence, for example. Hence, in both cases this radiation is isotropic. Conversely, in the near-edge or threshold region the process can be seen as a single two-step or higher order process, resonant Raman or resonant inelastic X-ray scattering, in which case the spectrum is energy-dependent and angle-dependent.

Having discussed the individual processes, in the next section we can now discuss the interaction of these processes in the quantum interference of X-ray absorption fine structure.

8. Quantum interference of the photoelectron and X-ray absorption fine structure

Photoionization emits a continuum electron in a near-spherical wave from the target orbital. The photoelectron scatters elastically and inelastically from the surrounding electron density. The backscattered photoelectron wave then interferes constructively and destructively at the origin, yielding the phenomenon of X-ray absorption fine structure (XAFS; Fig. 8).

This structure can be computed from the photoelectron scattering function, or equally and equivalently it can be formulated as the modulation of the photoionization event of the photon absorption. The presentation here is introductory in nature and leads to later chapters. Standard detailed derivations are given from different perspectives, much of this following from the work of Stern, Sayers and Lytle (Stern, 1974, 1988; Lee & Pendry, 1975; Ashley & Doniach, 1975; Durham, 1988). A number of presentations have gone beyond the simple XAFS equation, particularly in order to develop important software packages for real analysis (Gurman, 1988; Natoli *et al.*, 1990; Zabinsky *et al.*, 1995). Interesting introductions are given in several places (Mobilio, 2015; Bertoni, 2015; Fornasini, 2015; Benfatto & Meneghini, 2015; Kas *et al.*, 2016; Joly & Grenier, 2016). Other useful discussions and summaries are noted (Sayers *et al.*, 1970; Lytle *et al.*, 1975; Stern *et al.*, 1975; Rehr *et al.*, 1978, 1991; Lee *et al.*, 1981; Teo, 1981; Pendry, 1983; Durham, 1983; Rehr & Albers, 1990, 2000; de Leon *et al.*, 1991; Gurman, 1995).

The starting point of all presentations should be the perturbation theory photoabsorption cross section, amplitude, matrix element or form factor based on equations (43), (46), (49) and (51) for the development of perturbation theory expansions and equations (58), (59), (60), (64) and (65) for the perturbing time-dependent Hamiltonian. Some presentations of the multiple-scattering or XAFS interference provide only the first-order interference, whether representing the nearest-neighbour interference (Stern, 1974) or two shells, or two-path

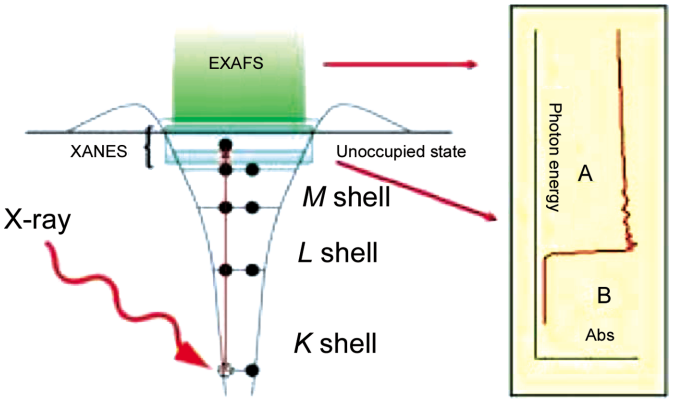

Figure 8
X-ray energy levels and the transitions leading to XAFS and XANES (X-ray absorption near-edge structure). Schematic representation of the interaction of a photon incident on an atom in a material. The atomic potential well is shown, as are the energy levels of the atomic shells. In this diagram the X-ray excites an electron from the *K* shell which can be promoted into unoccupied states in the vicinity of the *K* edge.

interference (Ashley & Doniach, 1975). Notice from the perturbation theory expansion that the sum in each order is over scattering from the whole potential, *i.e.* all paths and all electron density (subject to causality). However, the dominant contributions are the nearest nuclear potentials with the corresponding electron density for scattering, so that the second-order correction can include contributions from all two-leg paths: photoelectron scattering from nearest neighbours or more distant neighbours, from inner shells or further shells, while in third-order perturbation theory the sum is over all three-legged or triangular paths (scattering from one atom, then from another, then returning to the origin).

Hence in the history of the development of reviews of XAFS, early work used a point-scattering approximation corresponding to the atomic positions, while later work used plane waves and muffin-tin potentials centred at atomic positions (Lee & Pendry, 1975; Natoli *et al.*, 1990), curved waves (Gurman, 1988), curved waves to three legs and four legs and muffin-tin potentials centred at atomic sites (Lee & Pendry, 1975; Gurman *et al.*, 1986; Rehr & Albers, 1990), whereas in principle all electron density can contribute in each order. The transition rate and indeed the whole XAFS or XANES signal arises in lowest order in second-order perturbation theory (not first-order), or from the second term of the Born sequence, and may be compared with the 'atomic' or reference absorption coefficient without potential scattering of the photoelectron wave (the first-order cross section). Hence, a transition-matrix approach (Durham, 1983, 1988) requires and uses higher order perturbation theory. Similarly, the Green's function approaches and presentations (Ashley & Doniach, 1975; Rehr & Albers, 1990; Zabinsky *et al.*, 1995) do not expand the G_0 from the nonscattered probability (the lowest order) but collect the terms from multiple scattering arising from the higher order perturbation theory expansion, including the integral form for $G^{(+)}$. As such, the Green's function approaches and the multiple-scattering approaches are and must be isomorphic (Lee & Pendry, 1975), so that the major variations depend upon the approximations made to simplify the (relativistic) wavefunction and potential.

Following Lee & Pendry (1975) and Gurman *et al.* (1986), we comment that the primary functional fitted in XANES is $\mu(E)$ or $[\mu/\rho](\rho t)(E)$, whereas in all conventional XAFS or EXAFS fitting to date the relevant functional fitted is *ideally* $\chi(k)$,

$$\chi(k) = \frac{\left[\frac{\mu}{\rho}\right] - \left[\frac{\mu}{\rho}\right]_0}{\left[\frac{\mu}{\rho}\right]_0}. \tag{83}$$

In this equation it is assumed that all matrix attenuation and all attenuation by the nonresonant atoms and electrons has been removed, so that it is conventional to label this as isolating the atom and the electron for the relevant photoabsorption edge involved (for example the Ni K edge if resonant absorption is by a nickel inner-shell electron *etc.*) as *. Similarly, the theory directly relates only to photoabsorption coefficients, so any measured data would need in principle to correct for this to achieve amplitude ratios corresponding to the theoretical calculations. Hence,

$$\chi(k) = \frac{\left[\frac{\mu}{\rho}\right]^*_{\rm PE} - \left[\frac{\mu}{\rho}\right]^*_{\rm PE,0}}{\left[\frac{\mu}{\rho}\right]^*_{\rm PE,0}}. \tag{84}$$

Hence, $[\mu/\rho]^*_{\rm PE}$ is the contribution to the (measured) sample X-ray absorption that is attributed to the edge under consideration and $[\mu/\rho]^*_{\rm PE,0}$ is a smooth 'background' mass absorption corresponding to absorption by a free atom. In principle, the transmission measurement will only measure attenuation coefficients, including any signal loss due to elastic or inelastic scattering processes. Assuming, then, that the 'free-atom' background is the estimate without any interference channels, and hence is the prediction for photoabsorption of the first-order perturbation theory, with variations depending upon the integral over photoelectron energies and emitted solid angle and averaging over polarization as might be needed (from equations 58, 60, 64 and 65), we have to second order

$$\begin{aligned}
\left[\frac{\mu}{\rho}\right]_{\rm PE} &= \frac{1}{uA}\int_{\Omega_{\rm e},E'_{\rm e}} \frac{\hbar\omega P_{ij}}{I}\,{\rm d}\Omega_{\rm e}\,{\rm d}E'_{\rm e},\\
\frac{\hbar\omega P_{ij}}{I} &= \frac{\pi}{c\varepsilon_0\omega}\left|\left\langle j,e'\left|\frac{\hat{\mathbf{H}}'(t)}{A_0}\right|i\right\rangle\right.\\
&\quad \left. + \sum_k \frac{\left\langle j,e'\left|\frac{\hat{\mathbf{H}}'(t)}{A_0}\right|k\right\rangle\left\langle k|\hat{\mathbf{H}}'(t)|i\right\rangle}{E_j+E'_{\rm e}-E_i-\hbar\omega} + \ldots\right|^2\\
&\quad \times \delta(E_j+E'_{\rm e}-E_i-\hbar\omega),\\
\hat{\mathbf{H}}'(t) &\simeq A_0\frac{e}{m}\sum_i\left[\boldsymbol{\varepsilon}_{\mathbf{k}}\cdot\mathbf{p}_i\exp(i\mathbf{k}\cdot\mathbf{r}_i) + i\mathbf{S}_i\cdot\mathbf{k}\times\boldsymbol{\varepsilon}_{\mathbf{k}}\exp(i\mathbf{k}\cdot\mathbf{r}_i)\right.\\
&\quad \left. + \frac{eA'_0}{2}\exp(i\mathbf{K}\cdot\mathbf{r}_i)\left(\boldsymbol{\varepsilon}'_{\mathbf{k}}\cdot\boldsymbol{\varepsilon}_{\mathbf{k}} - i\frac{\hbar\omega}{mc^2}\mathbf{S}_i\cdot(\boldsymbol{\varepsilon}'_{\mathbf{k}}\times\boldsymbol{\varepsilon}_{\mathbf{k}})\right)\right],
\end{aligned} \tag{85}$$

$$\begin{aligned}
\left[\frac{\mu}{\rho}\right]_{\rm PE,0} &= \frac{1}{uA}\int_{\Omega_{\rm e},E'_{\rm e}} \frac{\hbar\omega P_{ij,0}}{I}\,{\rm d}\Omega_{\rm e}\,{\rm d}E'_{\rm e},\\
\frac{\hbar\omega P_{ij,0}}{I} &= \frac{\pi}{c\varepsilon_0\omega}\left|\left\langle j,e'\left|\frac{\hat{\mathbf{H}}'(t)}{A_0}\right|i\right\rangle\right|^2\delta(E_j+E'_{\rm e}-E_i-\hbar\omega).
\end{aligned} \tag{86}$$

It is normal, but not necessary, to then theoretically isolate the active subshell, implying the possibility of separating one electron, for example $|i,1s\rangle$, out of the full N electrons (or one subshell out of all subshells) or the independent electron approximation so that $|i\rangle = \Phi(i)^N = \Phi^{N-1}(i)\varphi^1(i)_{1s} = |(N-1)_i, (1s)_i\rangle$, implying antisymmetrization *etc.*, and similarly $\langle j,e'| = \Phi^\dagger(j)^{N-1}\Phi_{e'} = \langle(N-1)_j|\Phi_{e'}$ with an emitted photoelectron wavefunction. If one defines * for the active subshell as those processes only including an active transition involving the single core electron, with no interaction with the non-active-shell wavefunction, then this implies

$$\langle (N-1)_j | \frac{\hat{\mathbf{H}}'(t)}{A_0} | (N-1)_i \rangle = 0$$

and $\langle (N-1)_j || (N-1)_i \rangle = 1$. These (neglected) shake-up and shake-off processes are very significant near an edge, and are collective excitations with additional probabilities. They appear as contributions with shifted (higher) edge energies E_0' and have some amplitude and probability as a function of incident X-ray energy. These are very important in resonant inelastic X-ray scattering and related techniques. In standard XAFS analysis at higher energies above the edge, they can be approximated by a high-energy or impulse limit coefficient $S_0^2 = |\langle (N-1)_j || (N-1)_i \rangle|^2$. If considered as a higher order effect they can be included in the higher order perturbation theory and

$$\begin{aligned}
\left[\frac{\mu}{\rho}\right]^*_{\rm PE} &= \frac{1}{uA} \int_{\Omega_e, E_e'} \frac{\hbar\omega P_{ij}^*}{I} \, {\rm d}\Omega_e \, {\rm d}E_e' \\
\frac{\hbar\omega P_{ij}^*}{I} &= \frac{\pi}{c\varepsilon_0\omega} \left| \left\langle e' \left| \frac{\hat{\mathbf{H}}'(t)}{A_0} \right| i, 1s \right\rangle S_0 + \right. \\
&\quad \left. \sum_k \frac{\left\langle e' \left| \frac{\hat{\mathbf{H}}'(t)}{A_0} \right| k \right\rangle \langle k | \hat{\mathbf{H}}'(t) | i, 1s \rangle S_0^2}{E_j + E_e' - E_i - \hbar\omega} + \cdots \right|^2 \\
&\quad \times \delta(E_j + E_e' - E_i - \hbar\omega),
\end{aligned} \tag{87}$$

$$\begin{aligned}
\left[\frac{\mu}{\rho}\right]^*_{\rm PE,0} &= \frac{1}{uA} \int_{\Omega_e, E_e'} \frac{\hbar\omega P_{ij,0}}{I} \, {\rm d}\Omega_e \, {\rm d}E_e', \\
\frac{\hbar\omega P_{ij,0}^*}{I} &= \frac{\pi}{c\varepsilon_0\omega} \left| \left\langle e' \left| \frac{\hat{\mathbf{H}}'(t)}{A_0} \right| i, 1s \right\rangle \right|^2 S_0^2 \delta(E_j + E_e' - E_i - \hbar\omega).
\end{aligned} \tag{88}$$

The seagull (Thompson) and relativistic second-order spin terms are operators that are quadratic in $\mathbf{A}$, and hence impact upon scattering in the first-order perturbation theory term of equation (88). Conversely, terms that are first order in $\mathbf{A}$ are intrinsically photoabsorptive and thus only enter into scattering in the second-order perturbation term. Similarly, it is common in derivations to simplify the interaction (time-dependent) Hamiltonian to the electric dipole operator for the active electron following equation (64), whence $\hat{\mathbf{H}}'(t) \simeq A_0(e/m)\boldsymbol{\varepsilon}_\mathbf{k} \cdot \mathbf{p}_i \exp(i\mathbf{k} \cdot \mathbf{r}_i) \simeq A_0 e\hbar\omega_{ij}\boldsymbol{\varepsilon}_\mathbf{k} \cdot \mathbf{r}_i$. Notice that this neglects magnetic interactions, the seagull term and all higher order multipoles and selection rules. In this case, standard angular momentum probabilities may be determined following

$$\begin{aligned}
\frac{\hbar\omega P_{ij,0}^*}{I} &\simeq \frac{e^2\hbar^2\pi\omega_{ij}}{c\varepsilon_0} \left| \left\langle e' \left| \boldsymbol{\varepsilon}_\mathbf{k} \cdot \mathbf{r}_i \right| i, 1s \right\rangle \right|^2 S_0^2 \delta(E_j + E_e' - E_i - \hbar\omega), \\
&\simeq \frac{e^2\hbar^2\pi\omega_{ij}}{c\varepsilon_0} \sum_{m_i} \sum_{l'm'} \left| \left\langle l'm' \left| \boldsymbol{\varepsilon}_\mathbf{k} \cdot \mathbf{r}_i \right| l_i m_i \right\rangle \right|^2 \\
&\quad \times \exp(2i\delta_l) S_0^2 \delta(E_j + E_e' - E_i - \hbar\omega),
\end{aligned} \tag{89}$$

with a phase offset $\exp(2i\delta_l)$, where l_i, m_i are the angular momentum quantum numbers of the initial-state inner-shell electron, the sum being over degenerate sublevels of m_i; l', m' are the angular momentum quantum numbers associated with a term of the final-state wavefunction. For an isolated or independent electron approximation the final-state wavefunction, limited by selection rules, corresponds to the final state of the emitted photoelectron and can be written as a spherical wave and hence as a radial component multiplied by a spherical harmonic. As discussed, for example, in Lee & Pendry (1975), Gurman *et al.* (1986) and Gurman (1988), in an isolated atom *etc.* the matrix element is real so the central atom phase-shift factor can be factored out.

The next particular issue relates to the higher order scattering, especially of the photoelectron wave and the XAFS interference either for XANES or XAFS, following any of the standard derivations using the variations of constants, the U and T matrices or the Green's function formalism. Any higher order contribution can be due to any perturbation in the Hamiltonian, whether from the time-dependent photon field or indeed from the time-dependent propagation of the photoelectron wavefunction scattered from the surrounding potential. In the latter case, the higher order contribution in each order comes from a Green's function propagator to a scattering potential or electron density (for example at a muffin-tin atomic region), a T matrix to scatter the incoming (spherical) photoelectron wave to an outgoing (spherical) photoelectron wave and a Green's function propagator to propagate the outgoing photoelectron wave, ultimately back to the central atom where the photoemission occurred, to provide the interference term. Clearly, the sum of all of these higher order scattering terms in equation (86) can be denoted $\mathbf{Z}_{l'm';lm}$. As will be discussed further, this yields

$$\begin{aligned}
\chi(k) &= \frac{1}{\left[\frac{\mu}{\rho}\right]^*_{\rm PE,0}} \sum_{m_0} \sum_{lm;l'm'} \left\langle l_0 m_0 \left| \boldsymbol{\varepsilon}_\mathbf{k} \cdot \mathbf{r}_i \right| lm \right\rangle \\
&\quad \times 2{\rm Re}\mathbf{Z}_{lm;l'm'} \left\langle l'm' \left| \boldsymbol{\varepsilon}_\mathbf{k} \cdot \mathbf{r}_i \right| l_0 m_0 \right\rangle \exp[i(\delta_l + \delta_{l'})] S_0^2.
\end{aligned} \tag{90}$$

In earlier work, powerful agreement and support was obtained with only a few terms of the $\mathbf{Z}$ expansion into two-leg or other multiple-scattering paths, or indeed with only a few terms summed in the G expansion. More recently, experimental data have been observed to be sensitive to more paths, more legs and more contributions than previously contemplated, so that the expansion formalism is in fact very rich and will be explored in later chapters.

Perhaps to conclude this introductory presentation, and to point towards developments and derivations in later chapters, it will suffice to present forms for the standard XAFS equation for path (bond) distances R, coordination numbers N_R, structural and vibrational variance in path (bond) distances σ_R^2, the many-body amplitude-reduction factor (shake, satellite multi-electron processes) $S_0^2(k)$, the effective curved-wave backscattering amplitude $f_{\rm eff}(\theta_i, k, R) = |f_{\rm eff}(\theta_i, k, R)| \exp(i\Phi_{\rm eff})$ for an $(i+1)$-legged path, with $\theta_i = \pi$ for a two-legged path, the final-state l-wave central atom phase shift δ_c^l, the mean free

path of the photoelectron $\lambda(k)$ and the effective photoelectron wavenumber $k = \{[2m(E - E_0)]/\hbar^2\}^{1/2} \simeq 0.51235(E - E_0)^{1/2}$ with E in eV and k in Å^{-1}. Then, for s electron transitions (K edges, L_1 edges, M_1 edges, where the initial state has $l_0 = 0$, and dipole selection rules yield $l = l_0 + 1 = 1$) under these approximations

$$\begin{aligned}\chi_{l=0}(k) &\simeq -\sum_j N_j S_0^2(k) \frac{|f_{\rm eff}(\theta_i, k, r_j)|}{kr_j^2} \sin[2kr_j + \delta_j(k)^l + \Phi_{\rm eff}] \\ &\quad \times \exp(-2\sigma_j^2 k^2) \exp[-2r_j/\lambda(k), \delta_j(k)] \\ &= 2\delta_1 + \beta - \pi. \end{aligned} \tag{91}$$

For p electron transitions (L_2, L_3 edges and M_2, M_3 edges, where the initial state has $l_0 = 1$, and dipole selection rules yield $l = 0, 2$) under these approximations, we have two channels which interfere:

$$\begin{aligned}\chi_{l=1}(k) &\simeq -\sum_j N_j S_0^2(k) \frac{|f_{\rm eff}(\theta_i, k, r_j)|}{kr_j^2} \\ &\quad \times \left((1 - 3\cos^2\theta_j) M_{02} \sin[2kr_j + \delta'_{02j}(k)] \right. \\ &\quad \left. + \frac{1}{2}(1 + 3\cos^2\theta_j) \sin[2kr_j + \delta'_{2j}(k)] \right) \\ &\quad \times \exp(-2\sigma_j^2 k^2) \exp[-2r_j/\lambda(k)], \\ M_{02} &= |(\langle 2|z|1\rangle\langle 0|z|1\rangle + \langle 1|z|2\rangle\langle 1|z|0\rangle)\langle 2|z|1\rangle|^{-2}, \\ \delta'_{02j}(k) &= \delta_2(k) + \delta_0(k) + \beta_j(k). \end{aligned} \tag{92}$$

References

Åberg, T. & Tulkki, J. (1985). *Atomic Inner-Shell Physics*, edited by B. Crasemann, pp. 419–463. New York: AIP.

Arndt, U. W., Deslattes, R. D., Kessler, E. G. J., Indelicato, P., Lindroth, E., Creagh, D. C. & Hubbell, J. H. (1999). *International Tables for Crystallography*, Vol. C, edited by A. J. C. Wilson & E. Prince, pp. 191–258. Dordrecht: Kluwer Academic Publishers.

Ashley, C. A. & Doniach, S. (1975). *Phys. Rev. B*, **11**, 1279–1288.

Benfatto, M. & Meneghini, C. (2015). *Synchrotron Radiation: Basics, Methods and Applications*, edited by S. Mobilio, F. Boscherini & C. Meneghini, pp. 213–240. Berlin, Heidelberg: Springer.

Berestetskii, V. B., Lifshitz, E. M. & Pitaevskii, L. P. (1982). *Quantum Electrodynamics*, 2nd ed. Oxford: Butterworth-Heinemann.

Bertoni, C. M. (2015). *Synchrotron Radiation: Basics, Methods and Applications*, edited by S. Mobilio, F. Boscherini & C. Meneghini, pp. 145–178. Berlin, Heidelberg: Springer.

Blume, M. (1985). *J. Appl. Phys.* **57**, 3615–3618.

Blume, M. (1994). *Resonant Anomalous X-ray Scattering: Theory and Applications*, edited by G. Materlik, C. J. Sparks & K. Fischer, pp. 495–512. Amsterdam: North-Holland.

Born, M. & Wolf, E. (1980). *Principles of Optics*, 6th ed. Oxford: Pergamon Press.

Bransden, B. H. & Joachain, C. J. (1983). *Physics of Atoms and Molecules*. New York: Longman.

Chantler, C. T. (1994). *Resonant Anomalous X-ray Scattering: Theory and Applications*, edited by G. Materlik, C. J. Sparks & K. Fischer, pp. 61–78. Amsterdam: North-Holland.

Chantler, C. T. (1995). *J. Phys. Chem. Ref. Data*, **24**, 71–643.

Chantler, C. T. (2000). *J. Phys. Chem. Ref. Data*, **29**, 597–1056.

Chantler, C. T. (2024). *Int. Tables Crystallogr. I*, ch. 2.8, 88–99.

Chantler, C. T. & Creagh, D. C. (2024). *Int. Tables Crystallogr. C*. In the press.

Chantler, C. T., Lowe, J. A. & Grant, I. P. (2010). *Phys. Rev. A*, **82**, 052505.

Chantler, C. T., Smale, L. F. & Hudson, L. T. (2024). *Int. Tables Crystallogr. C*. In the press.

Compton, A. H. (1923*a*). *London Edinb. Dubl. Philos. Mag. J. Sci.* **45**, 1121–1131.

Compton, A. H. (1923*b*). *Phys. Rev.* **22**, 409–413.

Crasemann, B. (1996). *Atomic, Molecular and Optical Physics Handbook*, edited by G. W. F. Drake, pp. 701–711. New York: AIP.

Creagh, D. C. (1999). *International Tables for Crystallography*, Vol. C, edited by A. J. C. Wilson & E. Prince, pp. 242–258. Dordrecht: Kluwer Academic Publishers.

Creagh, D. C. & Chantler, C. T. (2024*a*). *Int. Tables Crystallogr. C*. In the press.

Creagh, D. C. & Chantler, C. T. (2024*b*). *Int. Tables Crystallogr. C*. In the press.

de Jonge, M. D., Tran, C. Q., Chantler, C. T., Barnea, Z., Dhal, B. B., Cookson, D. J., Lee, W. K. & Mashayekhi, A. (2005). *Phys. Rev. A*, **71**, 032702.

Delbrück, M. (1933). *Z. Phys.* **84**, 137.

Durham, P. J. (1983). *EXAFS and Near Edge Structure*, edited by A. Bianconi, L. Incoccia & S. Stipcich, pp. 37–43. Berlin, Heidelberg: Springer.

Durham, P. J. (1988). *X-ray Absorption: Principles, Applications, Techniques of EXAFS, SEXAFS and XANES*, pp. 53–84. New York: John Wiley & Sons.

Ericson, T. E. O. & Hüfner, J. (1973). *Nucl. Phys. B*, **57**, 604–616.

Fornasini, P. (2015). *Synchrotron Radiation: Basics, Methods and Applications*, edited by S. Mobilio, F. Boscherini & C. Meneghini, pp. 181–211. Berlin, Heidelberg: Springer.

Fujikawa, T. (2024). *Int. Tables Crystallogr. I*, ch. 2.5, 60–70.

Gerstenberg, H. & Hubbell, J. H. (1983). *Nuclear Data for Science and Technology*, edited by K. H. Böckhoff, pp. 1007–1009. Dordrecht: D. Reidel.

Glatzel, P., Juhin, A. & Moretti, M. (2024). *Int. Tables Crystallogr. I*, ch. 2.19, 177–189.

Grant, I. P. (1973). *Comput. Phys. Commun.* **5**, 263–282.

Grant, I. P. (2007). *Relativistic Quantum Theory of Atoms and Molecules: Theory and Computation*. New York: Springer.

Gurman, S. J. (1988). *J. Phys. C Solid State Phys.* **21**, 3699–3717.

Gurman, S. J. (1995). *J. Synchrotron Rad.* **2**, 56–63.

Gurman, S. J., Binsted, N. & Ross, I. (1986). *J. Phys. C Solid State Phys.* **19**, 1845–1861.

Hayward, E. (1993). *Radiat. Phys. Chem.* **41**, 739–749.

Hecht, E. & Zajac, A. (1979). *Optics*. Reading: Addison-Wesley.

Hubbell, J. H., Gimm, H. A. & Øverbø, I. (1980). *J. Phys. Chem. Ref. Data*, **9**, 1023–1148.

Jackson, J. D. (1975). *Classical Electrodynamics*, 2nd ed. New York: John Wiley & Sons.

James, R. W. (1962). *The Optical Principles of the Diffraction of X-rays*. London: Bell.

Joly, Y. & Grenier, S. (2016). *X-ray Absorption and X-ray Emission Spectroscopy*, edited by J. A. Bokhoven & C. Lamberti, pp. 73–97. Chichester: John Wiley & Sons.

Jönsson, P., Gaigalas, G., Bieroń, J., Fischer, C. F. & Grant, I. P. (2013). *Comput. Phys. Commun.* **184**, 2197–2203.

Kane, P. P., Kissel, L., Pratt, R. P. & Roy, S. C. (1986). *Phys. Rep.* **140**, 75–159.

Kas, J. J., Jorisson, K. & Rehr, J. J. (2016). *X-ray Absorption and X-ray Emission Spectroscopy*, edited by J. A. Bokhoven & C. Lamberti, pp. 51–72. Chichester: John Wiley & Sons.

Kissell, L. & Pratt, R. H. (1985). *Atomic Inner-Shell Physics*, edited by B. Crasemann, pp. 465–711. New York: AIP.

Klein, O. & Nishina, Y. (1929). *Z. Phys.* **52**, 853–868.

Laan, G. van der (2024). *Int. Tables Crystallogr. I*, ch. 2.18, 169–176.

Laan, G. van der & Figueroa, A. I. (2024). *Int. Tables Crystallogr. I*, ch. 2.17, 163–168.
Lee, P. A., Citrin, P. H., Eisenberger, P. & Kincaid, B. M. (1981). *Rev. Mod. Phys.* **53**, 769–806.
Lee, P. A. & Pendry, J. B. (1975). *Phys. Rev. B*, **11**, 2795–2811.
Loudon, R. (2000). *The Quantum Theory of Light*, 3rd ed. Oxford University Press.
Lowe, J. A., Chantler, C. T. & Grant, I. P. (2013). *Radiat. Phys. Chem.* **85**, 118–123.
Lytle, F. W., Sayers, D. E. & Stern, E. A. (1975). *Phys. Rev. B*, **11**, 4825–4835.
Milstein, A. I. & Schumacher, M. (1994). *Phys. Rep.* **243**, 183–214.
Mobilio, S. (2015). *Synchrotron Radiation: Basics, Methods and Applications*, edited by S. Mobilio, F. Boscherini & C. Meneghini, pp. 107–144. Berlin, Heidelberg: Springer.
Muckenheim, W. & Schumacher, M. (1980). *J. Phys. G Nucl. Phys.* **6**, 1237–1250.
Mustre de Leon, J., Rehr, J. J., Zabinsky, S. I. & Albers, R. C. (1991). *Phys. Rev. B*, **44**, 4146–4156.
Natoli, C. R., Benfatto, M., Brouder, C., López, M. F. R. & Foulis, D. L. (1990). *Phys. Rev. B*, **42**, 1944–1968.
Paolasini, L. & Di Matteo, S. (2024). *Int. Tables Crystallogr. I*, ch. 2.2, 41–47.
Papatzacos, P. & Mork, K. (1975). *Phys. Rev. D.* **12**, 206–218.
Pendry, J. B. (1983). *EXAFS and Near Edge Structure*, edited by A. Bianconi, L. Incoccia & S. Stipcich, pp. 4–10. Berlin, Heidelberg: Springer.
Pham, T. L. H., Nguyen, T. V. B., Lowe, J. A., Grant, I. P. & Chantler, C. T. (2016). *J. Phys. B At. Mol. Opt. Phys.* **49**, 035601.
Pratt, R. H., Kissel, L. & Bergstrom, P. M. Jr (1994). *Resonant Anomalous X-ray Scattering: Theory and Applications*, edited by G. Materlik, C. J. Sparks & K. Fischer, pp. 9–33. Amsterdam: North-Holland.
Rehr, J. J. & Albers, R. C. (1990). *Phys. Rev. B*, **41**, 8139–8149.
Rehr, J. J. & Albers, R. C. (2000). *Rev. Mod. Phys.* **72**, 621–654.
Rehr, J. J., Mustre de Leon, J., Zabinsky, S. I. & Albers, R. C. (1991). *J. Am. Chem. Soc.* **113**, 5135–5140.
Rehr, J. J., Stern, E. A., Martin, R. L. & Davidson, E. R. (1978). *Phys. Rev. B*, **17**, 560–565.
Rullhusen, P., Zurmühl, F., Smend, M., Schumacher, M., Börner, H. G. & Kerr, S. A. (1983). *Phys. Rev. C*, **27**, 559–568.
Sakurai, J. J. (1967). *Advanced Quantum Mechanics*. Reading: Addison-Wesley.
Sakurai, J. J. (1994). *Modern Quantum Mechanics*, revised ed. Reading: Addison-Wesley.
Sayers, D., Lytle, F. & Stern, E. (1970). *Adv. X-ray Anal.* **13**, 248–271.
Šipr, O. (2024). *Int. Tables Crystallogr. I*, ch. 2.16, 155–162.
Stern, E. A. (1974). *Phys. Rev. B*, **10**, 3027–3037.
Stern, E. A. (1988). *X-ray Absorption: Principles, Applications, Techniques of EXAFS, SEXAFS and XANES*, edited by D. C. Koningsberger & R. Prins, pp. 3–51. New York: John Wiley & Sons..
Stern, E. A., Sayers, D. E. & Lytle, F. W. (1975). *Phys. Rev. B*, **11**, 4836–4846.
Strutt, J. W. (1871). *Philos. Mag.* **41**, 447–454.
Teo, B. K. (1981). *EXAFS Spectroscopy: Techniques and Applications*, pp. 13–59. New York: Plenum.
Thomson, J. J. (1906). *Conduction of Electricity Through Gases*, 2nd ed. Cambridge University Press.
Thomson, J. J. & Thomson, G. P. (1933). *Conduction of Electricity Through Gases*, 3rd ed., Vol. II. Cambridge University Press.
Vettier, C. (1994). *Resonant Anomalous X-ray Scattering: Theory and Applications*, edited by G. Materlik, C. J. Sparks & K. Fischer, pp. 513–528. Amsterdam: North-Holland.
Wright, D. H. & Debevec, P. T. (1982). *Bull. Am. Phys. Soc.* **27**, 529.
Zabinsky, S. I., Rehr, J. J., Ankudinov, A., Albers, R. C. & Eller, M. J. (1995). *Phys. Rev. B*, **52**, 2995–3009.